

2020-01-01

Constitutive activation of the EGFRSTAT1 axis increases proliferation of meningioma tumor cells

Ferluga, S

<http://hdl.handle.net/10026.1/15873>

10.1093/noajnl/vdaa008

Neuro-Oncology Advances

Oxford University Press (OUP)

All content in PEARL is protected by copyright law. Author manuscripts are made available in accordance with publisher policies. Please cite only the published version using the details provided on the item record or document. In the absence of an open licence (e.g. Creative Commons), permissions for further reuse of content should be sought from the publisher or author.

[NOA-D-19-00065R2](#)

1 **Constitutive activation of the EGFR-STAT1 axis increases**
2 **proliferation of meningioma tumor cells**

3
4 **Sara Ferluga¹, Daniele Baiz¹, David A. Hilton², Claire L. Adams¹, Emanuela Ercolano¹, Jemma**
5 **Dunn¹, Kayleigh Bassiri¹, Kathreena M. Kurian³ and C. Oliver Hanemann^{1,4}**

6
7 ¹ University of Plymouth, Faculty of Health: Medicine, Dentistry and Human Sciences, The Institute of
8 Translational and Stratified Medicine, The John Bull Building, Plymouth Science Park, Research Way,
9 Plymouth UK, PL6 8BU

10 ² Cellular and Anatomical Pathology, Plymouth Hospitals NH Trust, Derriford Road, Plymouth UK, PL6
11 8DH

12 ³ Department of Neuropathology, Pathology Sciences, Southmead Hospital, Southmead Road, Bristol
13 UK, BS10 5NB

14 ⁴ **Corresponding author:** Prof. Clemens Oliver Hanemann MD, FRCP, Director of the Institute of
15 Translational and Stratified Medicine, University of Plymouth, Faculty of Health: Medicine, Dentistry and
16 Human Sciences, Plymouth Science Park, Research Way, Plymouth UK, PL6 8BU. Phone: +44
17 1752437418, Fax: +441752517846, E-mail: Oliver.Hanemann@plymouth.ac.uk

18
19 **Running Title:** EGFR-STAT1 tumor-promoting role in meningioma

20
21 **Funding:** This work was funded by Brain Tumour Research. DB was partially funded by the FP7 Marie
22 Curie Actions (PCOFUND-GA-20126001). Tissue samples were obtained from University Hospitals
23 Plymouth as part of the UK Brain Archive Information Network (BRAIN UK) which is funded by the
24 Medical Research Council.

25
26 **Conflict of Interest:** Authors declare that there are no conflicts of interest.

27
28 **Authorship:** Designing and execution of most of the experiments, data interpretation, manuscript and
29 figures preparation – SF

NOA-D-19-00065R2

30 Designing and execution of gene expression studies, data interpretation, writing of the related part,
31 performing experimental revisions and addressing comments to reviewers, proofreading of the
32 manuscript – DB

33 Designing and execution of immunohistochemistry, data interpretation, writing of the related part – DAH

34 Designing and execution of the flow cytometry experiments, data interpretation, writing of the related
35 part – CLA

36 Managing of tumor digestions and primary MN cells cultures – EE

37 Supporting with Western blot studies on MN Merlin status – JD

38 Supporting with the initial identification of STAT1 in meningioma – KB

39 Providing the majority of the samples involved in the study – KMK

40 Intellectual input to the critical design of the study, data interpretation, ~~proofreading of the~~ manuscript
41 preparation - COH

42

43 **Total Word Count: 60656217**

44

45

46

47

48

49

50 **Abstract**

51 **Background:** Meningiomas are the most frequent primary brain tumors of the central nervous system.
52 The standard of treatment is surgery and radiotherapy, but effective pharmacological options are not
53 available yet. The well-characterised genetic background stratifies these tumors in several subgroups,
54 thus increasing diversification. We identified EGFR-STAT1 overexpression and activation as a common
55 identifier of these tumors.

56 **Methods:** We analysed STAT1 overexpression and phosphorylation in 131 meningiomas of different
57 grades and locations by utilising several techniques, including Western blots, qPCR and
58 immunocytochemistry. We also silenced and overexpressed wild-type and mutant forms of the gene
59 to assess its biological function and its network. Results were further validated by drug testing.

60 **Results:** STAT1 was found widely overexpressed in meningioma but not in the corresponding healthy
61 controls. The protein showed a constitutive phosphorylation not dependent on the JAK/STAT pathway.
62 *STAT1* knock-down resulted in a significant reduction of cellular proliferation and deactivation of AKT
63 and ERK1/2. STAT1 is known to be activated by EGFR, so we investigated the tyrosine kinase and
64 found that EGFR was also constitutively phosphorylated in meningioma and was responsible for the
65 aberrant phosphorylation of STAT1. The pharmaceutical inhibition of EGFR caused a significant
66 reduction in cellular proliferation and of overall levels of Cyclin D1, pAKT and pERK1/2.

67 **Conclusions:** STAT1 EGFR-dependent constitutive phosphorylation is responsible for a positive
68 feedback loop that causes its own overexpression and consequently an increased proliferation of the
69 tumor cells. These findings provide the rationale for further studies aiming to identify effective
70 therapeutic options in meningioma.

71

72

73

74

75 **Keywords:** Meningioma, STAT1, EGFR, cancer, brain

76

77 **Importance of the Study**

78 Meningioma accounts for 37% of primary brain tumors. This year in the United States an estimated
79 thirty-two thousand people will be diagnosed with meningioma. ~~Despite the majority of~~ These tumors
80 ~~are benign in nature, they~~ can cause mild to severe morbidity and ~~even WHO grade I eventually~~
81 ~~progress to~~ can have a more aggressive ~~phenotype~~ clinical course. Therapeutic options are still limited
82 to surgical resection and radiotherapy since more effort is needed to decipher the communal molecular
83 mechanisms that define meningiomas despite their genetic background.

84 Aiming to discover novel therapeutic targets, we identified STAT1 as aberrantly overexpressed and
85 constitutively activated in most of the meningioma examined. Its activation is dependent on the
86 constitutive phosphorylation of EGFR and leads to an increased proliferation of tumor cells. We show
87 that specific EGFR inhibition can reduce tumor cell proliferation and we show evidence why previous
88 trials failed. Therefore, we suggest that this therapeutic strategy be re-evaluated.

89

90

91 Introduction

92 Meningiomas are the most common primary brain tumors, classified meningiomas as Grade I (~80%),
93 atypical Grade II (15-20%) and anaplastic/malignant Grade III (1-3%). Surgery is the primary choice of
94 treatment; complete resection may be curative but it can be achieved only for permissive locations¹.
95 The genetic background of meningioma is well characterised, with inactivation/deletion of *NF2* found in
96 ~60% of sporadic meningiomas².

97 Previously, we identified phosphorylated Signal Transducer and Activator of Transcription 1 (STAT1)
98 as overexpressed in the grade I meningioma cell line³ and phosphorylated STAT1 in meningioma tissue
99 of all grades⁴. In addition, we identified phosphorylation of STAT3 among remaining STAT family
100 members^{3,4}. STAT1 belongs to the STAT protein family that comprise seven members (STAT1-4,
101 STAT5A, STAT5B and STAT6), and it can be phosphorylated on the tyrosine 701 (Y701) and the serine
102 727 (S727)^{5,6}. STATs are essential components of the evolutionarily conserved JAK/STAT signalling
103 pathway^{4,7} that plays a role in immune response^{8,9} and its dysregulation is linked to cancer^{10,11}. This
104 canonical pathway is activated by ligands including interferons, interleukins and some growth factors,
105 binding to their receptors thus inducing phosphorylation of the JAKs (Janus Kinases), leading to ~~to~~
106 tyrosine-STAT phosphorylation by JAKs^{4,6}. In addition, STATs can also be phosphorylated by receptor
107 tyrosine kinases and cytoplasmic non-receptor tyrosine kinases⁵. Phosphorylated STATs homo- and
108 hetero-dimerize entering the nucleus to regulate transcription of target genes^{6,12}. JAKs include JAK1-3
109 and TYK2. JAK1 and JAK2 are phosphorylated following type-II interferon (IFN γ) stimulation, while
110 JAK1 and TYK2 are activated in type-I interferon signalling (IFN α , IFN β ; etc.)⁴⁻⁶. Activated JAK/STAT
111 pathway can be quenched by the SOCSs (Suppressors Of Cytokine Signalling), the PIASs (Protein
112 Inhibitors of Activated STAT) and the PTPs (Protein Tyrosine Phosphatases)⁵

113 Activated STAT1 acts as a transcriptional regulator, controlling its own transcription as well as the
114 expression of several IFN-regulated genes (IRGs)^{13,14}. STAT1 was considered a tumor suppressor as
115 its expression correlated with good prognosis in several types of cancer¹⁵⁻¹⁸. However, other studies
116 established a pro-tumorigenic role of STAT1, which correlated with its overexpression and activation¹⁹.
117 Due to its function in sensing and regulating cytokine production, STAT1 exerts a role in promoting an
118 immunosuppressive tumor environment^{19,20}. Hence, the overall role of STAT1 in cancer remains
119 complex suggesting that its function is most likely cancer type-dependent.

Formatted: Indent: First line: 0"

[NOA-D-19-00065R2](#)

In the present study, we identified STAT1 as overexpressed and phosphorylated in meningioma compared to normal and we show that its overexpression correlates with an increased proliferation of the tumor cells as well as an activation of AKT and ERK1/2. We demonstrate that STAT1 overexpression and phosphorylation is not dependent on the JAK/STAT pathway but it depends on a positive feedback loop caused by the constitutive activation of the Epidermal Growth Factor Receptor (EGFR). The pharmaceutical inhibition of EGFR in meningioma caused the deactivation of STAT1 and other cancer-related pathways, eventually leading to a significant reduction in cellular proliferation. Our findings underline a crucial role of the EGFR and STAT1 signalling in the pathology of meningiomas and point to a therapeutic potential of its inhibition.

Materials and Methods

Meningioma specimens, tumor digestion and primary meningioma cultures

Meningioma specimens were collected following the ethical approvals ([REC: 14/SW/0119; IRAS project ID: 153351; Plymouth Hospitals NHS Trust: R&D: 14/P/056, North Bristol NHS Trust: R&D: 3458](#)) received a unique MN number. ~~J specimens were collected via UK Brain Archive Information Network (BRAIN UK; Ref.:15/011; REC: 14/SG/0098) (Supplementary Table 1).~~ Normal meningeal tissue (NMT) [was purchased from Analytical Biological Service Inc.](#) ~~Primary cells were generated from 36 fresh t~~Tumor [tissues. Tissue](#) were disaggregated in DMEM with 15% FBS, 100 U/ml penicillin/streptomycin and 20 U/ml Collagenase III (Worthington Biochemical Corp) for 2 h at 37 °C; after cells were pelleted at 1000 rpm for 5 min, resuspended and seeded (modified from²¹). MN cells were cultured in DMEM at 37 °C in 5% CO₂. HMC cells (Caltag Medsystems Ltd) were grown in the recommended medium at 37 °C in 5% CO₂. [Cells were kept on average 4-5 passages.](#)

[Normal human meningeal cell were purchased from ScienceCell \(UK distributor: Caltag Medsystems; Catalog#1400\), U251 glioma cells were purchased from ECACC \(Cat n.: 09063001\), an immortalized grade 1 meningioma cell line BM-1 were \(DSMZ; Cat.n.: ACC 599\) and authenticated via genomic fingerprinting \(Eurofins Genomics Europe Applied Genomics GmbH\).](#)

Western blotting, immunofluorescence and immunohistochemistry

Western blots (WB) [from 26 frozen tissues and cell cultures](#) were performed as previously described³. All primary antibodies used are listed in Supplementary Table [42](#). Immunoreactive bands were quantified using Scion Image software and each band was normalized vs. the corresponding GAPDH.

Formatted: Font: 10 pt

Formatted: Normal, Left

Formatted: Font: 10 pt

Formatted: Font: 10 pt

Formatted: Font: 10 pt

NOA-D-19-00065R2

151 Immunofluorescence of 38 paraffin embedded tissue was performed as previously described³. Confocal
152 microscopy was executed using a Leica DMI6000B; Z-stack micrographs were taken using the 40X or
153 63X objectives. Immunofluorescent images for STAT1-silencing studies were taken with the Olympus
154 CKX41 with the 20X objective; images were processed with the QCapture Pro 6.0 software.

155 For immunohistochemistry, paraffin sections (4µm) were processed as described²². Avidin-biotin
156 blocking solution was used with EDTA pretreatment. Sections were incubated with appropriate biotin-
157 labelled secondary antibody and with horseradish peroxidase for detection using Vectashield Elite
158 (Vector Laboratories UK) according to the manufacturer's protocol. As a control, sections were
159 incubated with omission of the primary antibody.

160 Results were reviewed 'blind' to the histological grade by a neuropathologist (DAH). Semiquantitative
161 assessment of the intensity of immunoreactivity was undertaken and scored as follow: 0 none; 1 weak;
162 2 moderate; 3 strong.

RNA isolation and gene expression analysis

164 Total RNA was extracted from 95 frozen tissues and cells using the Qiazol® reagent (Qiagen UK),
165 following manufacturer's protocol. The quality, integrity and concentration of RNA were established
166 using the NanoDrop ND-2000 (ThermoFisher Scientific UK).

167 Real-Time PCR (qPCR) was conducted using 50 ng/well employing the EXPRESS One-Step SYBR®
168 GreenERTM kit (Invitrogen) on a LightCycler® 480 System (Roche Diagnostics, Switzerland), following
169 manufacturer's protocol (primers annealing temperature= 58 °C). Primers used were: PrimePCR™
170 SYBR® Green Assay STAT1 (BioRad), hGAPDH (2 µM, Invitrogen- Forward: 5'-
171 GAGAAGCTGGGGCTCATTT-3'; Reverse 5'-AGTGATGGCATGGACTGTGG-3'). Relative gene
172 expression analysis of STAT1 and GAPDH was calculated using the 2^{-ΔΔCt} method²³, employing the
173 HMC as calibrator.

STAT1 silencing and overexpression

174 Stat1 shRNA Lentiviral Particles (Santa Cruz Biotechnology, sc-44123-V), containing 3 target-specific
175 constructs that encode 19-25nt (plus hairpin) or scramble shRNA control (Santa Cruz Biotechnology,
176 sc-108080), were added onto the cells in media containing protamine sulfate salt (8 µg/ ml) (Sigma).
177 Cells were infected for 48 h before applying puromycin (5 µg/ml) for 3 days.

179 *STAT1-WT* gene was cloned into pCDNA3.1+ in a two-step process using the following primers:

180 STAT1-F1 (5'-AAAGCTAGCGGCCGGCCATGTCTCAG-3'), STAT1-R1 (5'-
181 CGTCTCGAGGTCAATTACCAAACCAGGCT-3') for the first part; STAT1-2F (5'-
182 GACCTCGAGACGACCTCTCT), STAT1-2R (5'-AGTGTTTAACTTAATTAACATACTGTGTTCA-3')

Formatted: Indent: First line: 0"

NOA-D-19-00065R2

183 for the second part. The 551 bp long STAT1 part in between the restriction sites HindIII and EcoRI was
184 synthesised (GeneArt, ThermoFisher Scientific) to generate the following mutations: Y701F, S727E and
185 Y701F/S727E; each one was cloned into pCDNA-STAT1-WT to replace the wild-type part. All
186 generated plasmids were sequenced before further use (Eurofins). U251-MG cells were transfected
187 and selected as previously described ²⁴.

Ki-67 staining and Proliferation assay

189 For Ki-67 staining, cells were grown on chamber slides, lentivirus-transfected and stained as previously
190 described³.

191 For U251-MG proliferation assay, the pool of U251-MG selected cells, transfected with pCDNA, STAT1-
192 WT and the three mutants, were seeded at 1000 cell/well in 96 well plates and proliferation was
193 determined after 24, 48 and 72 h using the 'CellTiter-Glo® Luminescent Cell Viability Assay' as
194 recommended by the supplier (Promega).

195 For drug testing, meningioma cells (~3000 cell/well) were plated in 96-well culture plates and allowed
196 to proliferate for 24 h. Cell proliferation was calculated as percentage of control cells. Graphs were
197 generated using GraphPad Prism 5.

Flow cytometry analysis

199 Confluent meningioma cells were resuspended in ice-cold staining buffer (PBS, 2%FBS) at a final
200 concentration of 1×10^5 cells. Cells were stained for 30 min at RT in the dark with the following: CD45-
201 FITC, HLA-DR-PE, CD14-PerCP5.5 and CD44 -APC (Becton Dickinson Biosciences, Pharmigen),
202 washed twice with 2 ml of staining buffer and centrifuged at 1500 rpm for 5 min at 4°C . The relevant
203 single isotype controls were used. Data acquisition was collected on 1×10^4 cells on a Accuri flow
204 cytometer (BD Biosciences) and analysis was performed using the Flow Jo software v10.0 (FlowJo
205 LLC, Ashland, OR).

Statistical analysis

207 Probability (p) values were calculated using the Student's t-Test or the ANOVA one-way analysis of
208 variance, using GraphPad Prism 5.01 and MS Excel 2016 software. P values <0.05 were considered
209 statistically significant. The results are expressed as means \pm SD or \pm SEM.

210

211

212

Formatted: Indent: First line: 0"

213

214

215 Results

216 STAT1 is overexpressed and aberrantly activated in meningioma

217

218 We analysed STAT1 expression in meningioma tumors compared to normal meninges (NMT). In all
219 cases STAT1 was overexpressed and in most of the cases, we detected high levels of phosphorylated
220 STAT1 (Y701 and S727) (representative Western blot of Fig. 1A and qPCR of Fig. 1C).
221 Immunohistochemical studies validated STAT1 overexpression in all meningioma samples (Fig. 1B);
222 also pSTAT1-Y701 and -S727 showed higher staining compared to normal meninges and an increasing
223 score throughout the grades. As control, we further analysed STAT1 and pSTAT1 abundance in two
224 additional normal meninges and a normal brain (Fig. 1D).

225 Then, we examined STAT1 expression and phosphorylation in meningioma-derived primary cells (MN)
226 and in BM-1²⁵ compared to HMC. MN cells were used between passage 3 and 5 and no B/T
227 lymphocytes or infiltrating macrophages were detected (Supplementary Fig. 1A). All cells were
228 vimentin-positive²⁶ and CD90-negative, suggesting no fibroblasts contamination²⁷ (Supplementary Fig.
229 1B). STAT1 was found overexpressed in BM-1 and MNs compared to HMC and both pSTAT1-Y701
230 and -S727 were present across all samples while faint and undetectable in HMC (Fig. 1C). Q-PCR
231 analysis confirmed that *STAT1* expression was higher in most of the MNs and in BM-1 compared to
232 control (Fig. 1F). Of note, STAT1 overexpression was independent of Merlin status (Supplementary Fig.
233 1C, D).

234 Furthermore, pSTAT1-Y701 showed a cytoplasmic localization while pSTAT1-S727 was nuclear (Fig.
235 1B), in agreement with the immunofluorescent staining of primary MN cells (Fig. 1G).

236 Overall, we examined 131 meningiomas vs. 10 normal meninges and 5 normal brains and we
237 demonstrate substantial overexpression of STAT1 in 100 of them with a variety of methods
238 (Supplementary Table 12).

239

240 STAT1 constitutive phosphorylation is not dependent on the JAK/STAT pathway

241 To further investigate STAT1 phosphorylation in the context of the tumor environment, we examined
242 meningioma tumor lysates for the presence of interferon gamma (IFN γ) and tumor-associated

Formatted: Indent: First line: 0"

NOA-D-19-00065R2

243 macrophages by using CD163 marker staining preferentially M2 macrophages²⁸. Variable protein
244 levels of IFN γ and CD163 were detected, but there was no evident correlation with STAT1
245 phosphorylation and no JAK1 phosphorylation was detected (Fig 2A).

246 STAT1 usually becomes phosphorylated as a result of JAK/STAT pathway activation in response to
247 external stimuli⁶. We examined whether STAT1 overexpression and phosphorylation was dependent
248 on the culture conditions and secreted factors. Culturing HMC in serum-free (SF) media and in BM-1
249 conditioned media, and BM-1 in SF media, we confirmed that STAT1 overexpression and
250 phosphorylation was not due to external factors, but most likely to an intrinsic activation (Fig. 2B).

251
252 Next, we decided to test the ability of the JAK/STAT pathway to respond to activating stimuli in
253 meningioma cells. HMC and two MNs were treated with IFN γ ; in HMC, JAK1 and JAK2 activated within
254 10 min after treatment as well as pSTAT1-Y701 whilst pSTAT1-S727 phosphorylated within 1 h. The
255 same behaviour was observed in MNs confirming that the JAK/STAT pathway was functional; however,
256 STAT1 was constitutively phosphorylated in non-treated cells while pJAK1 and pJAK2 were not (Fig.
257 2C). The same experiment, performed using interferon alpha (IFN α), produced comparable results
258 (Supplementary Fig. 2A).

259 After activation, pSTAT1 is known to dimerize and translocate into the nucleus⁶. IFN γ treatment was
260 indeed able to induce pSTAT1-Y701 nuclear internalization (Fig. 2D, Supplementary Fig. 2B). Thus,
261 the JAK/STAT1 pathway can be activated *via* IFN in meningioma cells but there was also an IFN-
262 independent intrinsic activation.

263 STAT1 constitutive phosphorylations could be due to a deficient deactivation of the pathway^{4,5,29}. Thus,
264 we analysed the levels of the SOCSs and the PIASs in HMC, BM-1 and MN cells (Fig. 2E), which did
265 not correlate with the constitutive phosphorylation of STAT1 observed in these samples (Fig. 1E).

266 Overall, these data suggest that the JAK/STAT pathway is functional but not over-activated. Therefore,
267 we hypothesized other mechanisms must be involved in maintaining STAT1 in a constitutive
268 phosphorylated form in the meningioma samples analyzed.

STAT1 overexpression is associated with an increased proliferation of meningioma cells

270
271 To investigate the biological significance of STAT1 overexpression in meningioma we silenced the
272 protein in MN cells. Lentiviral-mediated shRNA delivery into the cells produced an over 70% reduction
273 in protein expression (Fig. 3A) and a 50% reduction in gene expression levels compared to scramble

Formatted: Indent: First line: 0"

NOA-D-19-00065R2

274 (Fig. 3B). STAT1-silenced cells displayed a reduction in STAT1 immunofluorescent staining as well as
275 a reduction in Ki67-positive cells (Fig. 3C). Proliferating cells were reduced from ~22% to less than 5%
276 in MNs (Fig. 3D, E). This was in agreement with the reduction of the total number of cells (Fig. 3F) and
277 a 40% reduction of Cyclin D1 (Fig. 3A). A similar effect was observed in BM-1 cells (Supplementary Fig.
278 3A-D). Taken together, our results demonstrate that STAT1 overexpression is associated to an
279 increased proliferation of meningioma tumor cells.

280 The MAPK-ERK and the AKT pathways are known to be active in meningioma and to influence tumor
281 progression³⁰. After STAT1-KD, both AKT and ERK1/2 showed a 95% and 80% reduction in protein
282 phosphorylation respectively (Fig. 3G, H), supporting a critical involvement of STAT1 in the activation
283 of pro-proliferative pathways.

284

Phosphorylated STAT1 affects activation of AKT and ERK1/2 and cellular proliferation

286 We used phosphomimetics to further characterise the effects of STAT1 phosphorylation. Phenylalanine
287 (F) and Glutamic acid (E) are used to mimic the structure of a phosphorylated tyrosine (Y) and
288 phosphorylated serine (S) respectively³¹. We produced three different STAT1 mutants: Y701F, S727E
289 and the double mutant Y701F/S727E. Since STAT1 is constitutively phosphorylated in meningioma, we
290 used U251-MG cells as a model because this cell line showed levels of total and pSTAT1 lower than
291 HMC (Fig. 4A). STAT1 overexpression in U251-MG for wild-type (WT) and mutants was confirmed by
292 WB and qPCR (Fig. 4B, C). STAT1 overexpression in U251-MG cells determined an increased
293 phosphorylation of AKT and ERK1/2, where the effect was particularly evident for pERK1/2 in STAT1-
294 S727E and STAT1-Y701F/S727E mutants (Fig. 4B).

295 The proliferation of transfected cells was measured over a period of 72 h and normalised for the empty-
296 vector control. All STAT1 mutants showed a significantly increased proliferation rate compared to
297 STAT1-WT; interestingly, the double mutant STAT1- Y701F/S727E, which represents STAT1 in its
298 maximal activated condition, determined the highest pro-proliferative effect in U251-MG cells (Fig. 4B,
299 4D).

300 These experiments confirmed that the constitutive phosphorylation of STAT1 on both phosphosites
301 affects the activation of the AKT and ERK1/2 pathways as well as the proliferation of the cells in
302 agreement with STAT1 knock-down results in meningioma.

303

EGFR constitutive phosphorylation is responsible for STAT1 overexpression and activation

Formatted: Indent: First line: 0"

Formatted: Indent: First line: 0"

[NOA-D-19-00065R2](#)

305 It has been previously shown that STAT1 can be phosphorylated by EGFR, a key tyrosine kinase
306 relevant to the majority of tumors^{32,33}. We examined the EGFR status in meningioma tissues and cells,
307 detecting high levels of pEGFR in both tumor lysates and meningioma cells, when compared to normal
308 meningeal tissue (NMT) and HMC (Fig. 5A).

309 To test whether the constitutive phosphorylation of EGFR was responsible for STAT1 phosphorylation,
310 we treated BM-1 cells with three different EGFR inhibitors (canertinib andafatinib, 2nd generation
311 irreversible inhibitors) and erlotinib (1st generation, reversible inhibitor), , for 30 min, 3, 6 and 24 h³⁴.
312 Canertinib (and similarly afatinib) decreased STAT1 expression of about 60% within 24 h upon;
313 pSTAT1-Y701 was almost abolished 30 min after treatment but was restored at 24 h while pSTAT1-
314 S727 showed a decrease of about 90% compared to vehicle at 24 h (Fig. 5B). Almost no effect on total
315 and pSTAT1 was detected after treatment with erlotinib, which did not cause an evident decrease in
316 pEGFR-Y1068 after treatment (Fig. 5B).

317 EGFR blockade *via* canertinib and afatinib decreased pSTAT1 levels and determined a concentration-
318 dependent decrease of cellular proliferation already at 24 h after treatment (Fig. 5C), with erlotinib being
319 ineffective.

320 Since canertinib showed the strongest effect on STAT1 in BM-1 cells, we tested its effects on primary
321 MNs (Fig. 5D). Canertinib was active in reducing EGFR constitutive phosphorylation in MN cells,
322 reducing p-STAT1 levels after canertinib treatment; pSTAT1-S727 reduced of 65% already 3 h after
323 treatment and stayed low over the 24 h; phosphorylated STAT1-Y701 also showed about 50% reduction
324 3 h after treatment and recovered between 6 and 24 h (Fig. 5D, E Supplementary Fig. 4).

325 Phospho-AKT and pERK1/2 showed a decrease of about 70% and Cyclin D1 reduced to 50% in 24 h
326 (Fig. 5D,E,Supplementary Fig. 4).

327 We wanted to examine whether the inhibition of pEGFR and thus of pSTAT1 had any effect on *STAT1*
328 expression, as STAT1 is known to regulate its own transcription³⁵. *STAT1* expression levels reduced
329 by ~50% 24 h after treatment with canertinib in MNs (Fig. 5F), consistently with a 30% reduction in
330 protein level observed by WB analysis (Fig. 5D, E, Supplementary Fig. 4).

331 Lastly, to confirm the link between EGFR activation and STAT1 phosphorylation, we treated BM-1 cells
332 with the Epidermal Growth Factor (EGF) for 5, 30 and 60 minutes. Upon EGF treatment STAT1 was
333 phosphorylated on Y701 within 5 minutes and on S727 within 30 minutes (Fig. 5G).

334 Hence, we showed that EGFR is responsible for STAT1 overexpression and constitutive activation in
335 meningioma, which consequently increases proliferation of the tumor cells.

Formatted: Indent: First line: 0"

336

337

338

339

340

341

342 Discussion

343 Meningiomas are the most common primary brain tumor but there are no therapeutic options available
344 other than surgery and radiotherapy^{1,36}. The well-defined genetic background of meningioma is leading
345 towards an increasing stratification of these tumors into subtypes^{37,38}; however, common features
346 should still be investigated.

347 We identified STAT1 as overexpressed and activated in 84% of meningioma examined. The only
348 study exploring the expression levels of STAT and JAK superfamilies in meningiomas was published
349 in 1999 showing higher immunoreactivity of JAK1 (see also Supplementary Fig. 2C), JAK2 and the
350 STATs in meningiomas compared to normal dura³⁹. Our data confirmed the expression of the JAKs in
351 MN cells and in HMC; we showed that the JAK/STAT pathway is activated by IFN α and IFN γ , inducing
352 nuclear localization of pSTAT1 as seen before³⁹. As previously reported⁴⁰, activation of STAT1
353 after INF γ stimulation occurs via JAK kinases by phosphorylation on Y701, resulting in
354 pSTAT1 translocation into the nucleus and subsequent phosphorylation at S727⁴¹. Double
355 phosphorylation is required for maximal STAT1 activity. However, we show that STAT1 is
356 constitutively phosphorylated in MNs but not in HMC, even without IFN stimulation and in serum-free
357 conditions. In tumor lysates, STAT1 phosphorylation was not consistent with the presence of M2-
358 polarised macrophages or IFN γ suggesting that the constitutive activation of STAT1 was not related to
359 the JAK/STAT pathway.

360 To better understand the meaning of this STAT1 phosphorylation we used phosphomimetics,
361 generating STAT1-Y701F, STAT1-S727E and STAT1-Y701F/S727E mutants. The overexpression of
362 these mutants induced activation of two central nodes in cancer signalling, AKT and ERK1/2, and

Formatted: Left, Indent: First line: 0", Don't adjust space between Latin and Asian text, Don't adjust space between Asian text and numbers

Formatted: Indent: First line: 0"

[NOA-D-19-00065R2](#)

363 increased cellular proliferation. A similar approach was used on STAT3 in human prostate cancer cell,
364 where the mutant STAT3-Y705F/S727E promoted survival, growth and invasion. They showed that the
365 mutation S727E was increasing the transcription of c-Myc, which is an essential activator of cell growth
366 and proliferation³¹. It is very likely that a similar mechanism is happening also in meningioma, where
367 STAT1-S727 showed a predominant nuclear localization exerting its role of transcriptional regulator.

368 We also showed the link between STAT1 overexpression and the increased proliferation of the tumor
369 cells. This effect is most likely linked to an activating cascade involving ERK1/2 and AKT, since their
370 activated state and cell proliferation were almost aborted after STAT1 silencing. The activation of the
371 MAPK pathway is involved in both proliferation and apoptosis in meningioma³⁰, and we recently
372 published a proteomic profiling of meningioma, identifying the aberrant activation of the PI3K/AKT
373 pathway across all meningioma grades⁴.

374 Aiming to identify the kinase responsible for STAT1 activation, we examined the status of EGFR, a
375 tyrosine kinase able to phosphorylate STAT1^{33,42,43}. EGFR was overexpressed and constitutively
376 phosphorylated on Y1068 in all of the MN cells examined but not in HMC. To test whether EGFR
377 phosphorylation was responsible for the constitutive activation of STAT1 we used three specific EGFR
378 inhibitors canertinib, afatinib and erlotinib⁴⁴. Whilst canertinib and afatinib, had a similar effect in
379 reducing STAT1 phosphorylation on both phosphosites as well as on cell proliferation and viability,
380 erlotinib, did not produce any significant effect. Interestingly this result is consistent with the
381 unsuccessful clinical trial of erlotinib on recurrent meningiomas⁴⁵. Erlotinib is a first generation ATP
382 dependent reversible rather broad inhibitor⁴⁶, Afinitinib and Canertinib are non reversible second
383 generation with high pEC50 <https://www.proteomicsdb.org/#analytics/selectivity>

384 In MN cells, canertinib (and afatinib) caused the de-phosphorylation of STAT1-Y701 and S&27 within
385 6 and 24H respectively. Similarly, EGF stimulation induces an immediate and direct phosphorylation on
386 Y701 and a later one on S727, suggesting the activation of an additional kinase downstream of EGFR,
387 which is probably part of the MAPK/ERK1/2 pathway⁴⁷. Indeed previous studies in pancreatic cancer
388 demonstrated the relationship between EGFR and the downstream signalling regulators like pAKT,
389 pERK1/2 and Cyclin D1³³. In agreement, after canertinib treatment and after STAT1 silencing, we
390 observed a significant reduction of pAKT and pERK1/2. Overall, levels of Cyclin D1 also displayed a
391 significant reduction, consistently with the reduction in proliferation observed after STAT1 silencing and
392 canertinib treatment.

NOA-D-19-00065R2

393 The observed reduction in STAT1 expression suggest a feedback regulatory mechanism of pSTAT1 on
394 its own promoter, already documented³⁵, as well as an EGFR/HER2-dependent regulation as previously
395 shown in glioblastoma and breast cancer cell lines⁴⁸.

396 In conclusion, we provide clear evidence of STAT1 overexpression in meningioma of different genotype
397 and its correlation with an increased cellular proliferation. We demonstrate that STAT1 is aberrantly
398 phosphorylated on both phosphosites, not because of the JAK/STAT pathway activation but because
399 of the constitutive phosphorylation of EGFR, which elicits activation of the MAPK/ERK and PI3K/AKT
400 pathways and an increase in the overall levels of Cyclin D1 and STAT1. Although the whole mechanism
401 should be additionally studied to give a thorough understanding of the activating cascade and all the
402 partners involved in it, our studies set the basis for re-evaluating EGFR inhibition in meningioma as
403 possible therapeutic option.

Formatted: Indent: First line: 0"

404 **References**

- 405 1. Whittle IR, Smith C, Navoo P, Collie D. Meningiomas. *Lancet*. 2004; 363(9420):1535-
406 1543.
- 407 2. Suppiah S, Nassiri F, Bi WL, et al. Molecular and translational advances in
408 meningiomas. *Neuro Oncol*. 2019; 21(Supplement_1):i4-i17.
- 409 3. Bassiri K, Ferluga S, Sharma V, et al. Global Proteome and Phospho-proteome
410 Analysis of Merlin-deficient Meningioma and Schwannoma Identifies PDLIM2 as a
411 Novel Therapeutic Target. *EBioMedicine*. 2017; 16:76-86.
- 412 4. Dunn J, Ferluga S, Sharma V, et al. Proteomic analysis discovers the differential
413 expression of novel proteins and phosphoproteins in meningioma including NEK9,
414 HK2 and SET and deregulation of RNA metabolism. *EBioMedicine*. 2018.
- 415 5. Lee M, Rhee I. Cytokine Signaling in Tumor Progression. *Immune Netw*. 2017;
416 17(4):214-227.
- 417 6. Kiu H, Nicholson SE. Biology and significance of the JAK/STAT signalling pathways.
418 *Growth Factors*. 2012; 30(2):88-106.
- 419 7. O'Shea JJ, Schwartz DM, Villarino AV, Gadina M, McInnes IB, Laurence A. The JAK-
420 STAT pathway: impact on human disease and therapeutic intervention. *Annu Rev*
421 *Med*. 2015; 66:311-328.
- 422 8. van de Veerdonk FL, Plantinga TS, Hoischen A, et al. STAT1 mutations in autosomal
423 dominant chronic mucocutaneous candidiasis. *N Engl J Med*. 2011; 365(1):54-61.
- 424 9. Holland SM, DeLeo FR, Elloumi HZ, et al. STAT3 mutations in the hyper-IgE
425 syndrome. *N Engl J Med*. 2007; 357(16):1608-1619.
- 426 10. You Z, Xu D, Ji J, Guo W, Zhu W, He J. JAK/STAT signal pathway activation
427 promotes progression and survival of human oesophageal squamous cell carcinoma.
428 *Clin Transl Oncol*. 2012; 14(2):143-149.
- 429 11. Tu Y, Zhong Y, Fu J, et al. Activation of JAK/STAT signal pathway predicts poor
430 prognosis of patients with gliomas. *Med Oncol*. 2011; 28(1):15-23.
- 431 12. Lillemeier BF, Koster M, Kerr IM. STAT1 from the cell membrane to the DNA. *EMBO*
432 *J*. 2001; 20(10):2508-2517.
- 433 13. Kohanbash G, Okada H. MicroRNAs and STAT interplay. *Semin Cancer Biol*. 2012;
434 22(1):70-75.
- 435 14. Ramana CV, Chatterjee-Kishore M, Nguyen H, Stark GR. Complex roles of Stat1 in
436 regulating gene expression. *Oncogene*. 2000; 19(21):2619-2627.
- 437 15. Simpson JA, Al-Attar A, Watson NF, Scholefield JH, Ilyas M, Durrant LG.
438 Intratumoral T cell infiltration, MHC class I and STAT1 as biomarkers of good
439 prognosis in colorectal cancer. *Gut*. 2010; 59(7):926-933.
- 440 16. Chen G, Wang H, Xie S, Ma J, Wang G. STAT1 negatively regulates hepatocellular
441 carcinoma cell proliferation. *Oncol Rep*. 2013; 29(6):2303-2310.
- 442 17. Sun Y, Yang S, Sun N, Chen J. Differential expression of STAT1 and p21 proteins
443 predicts pancreatic cancer progression and prognosis. *Pancreas*. 2014; 43(4):619-
444 623.
- 445 18. Schneckeleithner C, Bago-Horvath Z, Dolznig H, et al. Putting the brakes on
446 mammary tumorigenesis: loss of STAT1 predisposes to intraepithelial neoplasias.
447 *Oncotarget*. 2011; 2(12):1043-1054.
- 448 19. Meissl K, Macho-Maschler S, Muller M, Strobl B. The good and the bad faces of
449 STAT1 in solid tumours. *Cytokine*. 2017; 89:12-20.
- 450 20. Hix LM, Karavitis J, Khan MW, Shi YH, Khazaie K, Zhang M. Tumor STAT1
451 transcription factor activity enhances breast tumor growth and immune suppression
452 mediated by myeloid-derived suppressor cells. *J Biol Chem*. 2013; 288(17):11676-
453 11688.
- 454 21. James MF, Lelke JM, Maccollin M, et al. Modeling NF2 with human arachnoid and
455 meningioma cell culture systems: NF2 silencing reflects the benign character of
456 tumor growth. *Neurobiol Dis*. 2008; 29(2):278-292.
- 457 22. Hilton DA, Ristic N, Hanemann CO. Activation of ERK, AKT and JNK signalling
458 pathways in human schwannomas in situ. *Histopathology*. 2009; 55(6):744-749.

Formatted: German (Germany)

NOA-D-19-00065R2

- 459 23. Livak KJ, Schmittgen TD. Analysis of relative gene expression data using real-time
460 quantitative PCR and the 2(-Delta Delta C(T)) Method. *Methods*. 2001; 25(4):402-
461 408.
- 462 24. Ferluga S, Hantgan R, Goldgur Y, Himanen JP, Nikolov DB, Debinski W. Biological
463 and structural characterization of glycosylation on ephrin-A1, a preferred ligand for
464 EphA2 receptor tyrosine kinase. *J Biol Chem*. 2013; 288(25):18448-18457.
- 465 25. Puttmann S, Senner V, Braune S, et al. Establishment of a benign meningioma cell
466 line by hTERT-mediated immortalization. *Lab Invest*. 2005; 85(9):1163-1171.
- 467 26. Schweddeheimer K, Kartenbeck J, Moll R, Franke WW. Vimentin filament-desmosome
468 cytoskeleton of diverse types of human meningiomas. A distinctive diagnostic
469 feature. *Lab Invest*. 1984; 51(5):584-591.
- 470 27. Sorrell JM, Caplan AI. Fibroblasts-a diverse population at the center of it all. *Int Rev*
471 *Cell Mol Biol*. 2009; 276:161-214.
- 472 28. Komohara Y, Horlad H, Ohnishi K, et al. M2 macrophage/microglial cells induce
473 activation of Stat3 in primary central nervous system lymphoma. *J Clin Exp Hematop*.
474 2011; 51(2):93-99.
- 475 29. Seif F, Khoshmirsafa M, Aazami H, Mohsenzadegan M, Sedighi G, Bahar M. The
476 role of JAK-STAT signaling pathway and its regulators in the fate of T helper cells.
477 *Cell Commun Signal*. 2017; 15(1):23.
- 478 30. Mawrin C, Sasse T, Kirches E, et al. Different activation of mitogen-activated protein
479 kinase and Akt signaling is associated with aggressive phenotype of human
480 meningiomas. *Clin Cancer Res*. 2005; 11(11):4074-4082.
- 481 31. Qin HR, Kim HJ, Kim JY, et al. Activation of signal transducer and activator of
482 transcription 3 through a phosphomimetic serine 727 promotes prostate
483 tumorigenesis independent of tyrosine 705 phosphorylation. *Cancer Res*. 2008;
484 68(19):7736-7741.
- 485 32. Tong J, Taylor P, Moran MF. Proteomic analysis of the epidermal growth factor
486 receptor (EGFR) interactome and post-translational modifications associated with
487 receptor endocytosis in response to EGF and stress. *Mol Cell Proteomics*. 2014;
488 13(7):1644-1658.
- 489 33. Seshacharyulu P, Ponnusamy MP, Rachagani S, et al. Targeting EGF-receptor(s) -
490 STAT1 axis attenuates tumor growth and metastasis through downregulation of
491 MUC4 mucin in human pancreatic cancer. *Oncotarget*. 2015; 6(7):5164-5181.
- 492 34. Roskoski R, Jr. ErbB/HER protein-tyrosine kinases: Structures and small molecule
493 inhibitors. *Pharmacol Res*. 2014; 87:42-59.
- 494 35. Yang J, Stark GR. Roles of unphosphorylated STATs in signaling. *Cell Res*. 2008;
495 18(4):443-451.
- 496 36. Moazzam AA, Wagle N, Zada G. Recent developments in chemotherapy for
497 meningiomas: a review. *Neurosurg Focus*. 2013; 35(6):E18.
- 498 37. Brastianos PK, Horowitz PM, Santagata S, et al. Genomic sequencing of
499 meningiomas identifies oncogenic SMO and AKT1 mutations. *Nat Genet*. 2013;
500 45(3):285-289.
- 501 38. Clark VE, Harmanci AS, Bai H, et al. Recurrent somatic mutations in POLR2A define
502 a distinct subset of meningiomas. *Nat Genet*. 2016; 48(10):1253-1259.
- 503 39. Magrassi L, De-Fraja C, Conti L, et al. Expression of the JAK and STAT
504 superfamilies in human meningiomas. *J Neurosurg*. 1999; 91(3):440-446.
- 505 40. Khodarev NN, Roizman B, Weichselbaum RR. Molecular pathways: interferon/stat1
506 pathway: role in the tumor resistance to genotoxic stress and aggressive growth. *Clin*
507 *Cancer Res*. 2012; 18(11):3015-3021.
- 508 41. Sadzak I, Schiff M, Gattermeier I, et al. Recruitment of Stat1 to chromatin is required
509 for interferon-induced serine phosphorylation of Stat1 transactivation domain. *Proc*
510 *Natl Acad Sci U S A*. 2008; 105(26):8944-8949.
- 511 42. Petschnigg J, Groisman B, Kotlyar M, et al. The mammalian-membrane two-hybrid
512 assay (MaMTH) for probing membrane-protein interactions in human cells. *Nat*
513 *Methods*. 2014; 11(5):585-592.
- 514 43. Collins-McMillen D, Stevenson EV, Kim JH, et al. HCMV utilizes a non-traditional
515 STAT1 activation cascade via signaling through EGFR and integrins to efficiently

Formatted: German (Germany)

Formatted: German (Germany)

| [NOA-D-19-00065R2](#)

- 516 promote the motility, differentiation, and polarization of infected monocytes. *J Virol.*
517 2017.
- 518 **44.** Smaill JB, Rewcastle GW, Loo JA, et al. Tyrosine kinase inhibitors. 17. Irreversible
519 inhibitors of the epidermal growth factor receptor: 4-(phenylamino)quinazoline- and 4-
520 (phenylamino)pyrido[3,2-d]pyrimidine-6-acrylamides bearing additional solubilizing
521 functions. *J Med Chem.* 2000; 43(7):1380-1397.
- 522 **45.** Norden AD, Raizer JJ, Abrey LE, et al. Phase II trials of erlotinib or gefitinib in
523 patients with recurrent meningioma. *J Neurooncol.* 2010; 96(2):211-217.
- 524 **46.** Conradt L, Godl K, Schaab C, et al. Disclosure of erlotinib as a multikinase inhibitor
525 in pancreatic ductal adenocarcinoma. *Neoplasia.* 2011; 13(11):1026-1034.
- 526 **47.** Vanhatupa S, Ungureanu D, Paakkunainen M, Silvennoinen O. MAPK-induced
527 Ser727 phosphorylation promotes SUMOylation of STAT1. *Biochem J.* 2008;
528 409(1):179-185.
- 529 **48.** Han W, Carpenter RL, Cao X, Lo HW. STAT1 gene expression is enhanced by
530 nuclear EGFR and HER2 via cooperation with STAT3. *Mol Carcinog.* 2013;
531 52(12):959-969.

532

533 **Figure Legends**

534

535 **Fig. 1** STAT1 and its phosphorylated forms are overexpressed in meningioma. **A** Representative WB
536 analysis showing the expression of total and pSTAT1 in different grade meningiomas vs. NMT **B**
537 Representative images showing the IHC staining of STAT1 and pSTAT1 in the three grades
538 meningiomas compared to normal meninges (see black arrows) at 200X magnification. Mean scores
539 are presented in the table below for the specimens and the normal controls examined (see also
540 Supplementary Table [21](#) for the full list of specimens examined and the corresponding scores – n=47).
541 **C** *STAT1* expression levels in WHO I (n=40), WHO II (n=25) and WHO III (n= 10) meningioma tumors
542 normalised vs. [normal meningeal tissue \(NMT\)](#). Data are presented as mean \pm SEM; * = $p \leq 0.05$. **D**
543 WB showing pSTAT1 and STAT1 in normal brain (NB) and additional normal meninges (NMT-1 and
544 NMT-2) compared to sample J6 (meningioma) as positive control. **E** Representative WB analysis of
545 STAT1 and pSTAT1 in BM-1 and in WHO I MN cells (MNs) vs. HMC. **F** *STAT1* expression levels in
546 BM-1 (n=4) and in MN cells (n=24) normalised vs. HMC. Data are presented as mean \pm SEM; ** = $p \leq$
547 0.01. **E G** Confocal z-stack images showing the immunofluorescent staining of STAT1 (red) and
548 pSTAT1 (Y701- green and S727- red) in MN cells vs. HMC. Scale bar 50- μ m. Nuclei were stained with
549 DAPI (blue).

[NOA-D-19-00065R2](#)

550 **Fig. 2** STAT1 phosphorylation in meningioma cells is not dependent on the JAK/STAT pathway. **A** WB
551 of WHO I meningioma tumor tissue lysates (n=8); the presence of gamma interferon (IFN γ) and
552 macrophage infiltration (CD163) into the tumor were analysed in relation to STAT1 and pSTAT1 levels.
553 Phospho-JAK1 was used to detect activation of the JAK-STAT pathway (*=positive control for pJAK1
554 antibody. **B**). WB of total and pSTAT1 in BM-1 and HMC cells, grown in different culture condition. HMC:
555 HMC cells media; MN: MN cells media; MN-SF: MN-serum free media; MN-SF+FBS: MN serum free
556 for 24 h + FBS for 24h; MN Cond: meningioma cells-conditioned media **C** WB analysis of STAT1 and
557 pSTAT1 protein levels in HMC and two primary MN cells after IFN γ treatment at the concentration of 50
558 ng/ml for the indicated amount of time. Phospho-JAK1 and pJAK2 are shown to confirm the activation of
559 the JAK/STAT pathway. **D** Representative confocal images (z-stack) showing localization of pSTAT1-
560 Y701 (green) and pSTAT1-S727 (red) in primary MN cells before and after IFN γ stimulation (50 ng/ml
561 for 1 h). Scale bar 50- μ m. Nuclei were stain with DAPI (blue). **E** WB analysis of SOCSs and PIASs
562 protein levels in BM-1 and primary MNs compared to HMC.

[NOA-D-19-00065R2](#)

563 **Fig. 3** STAT1 overexpression increases meningioma cells proliferation. **A** Histogram representing the
564 percentage of statistical reduction in STAT1 and Cyclin D1 protein levels after *STAT1* sh-RNA-mediated
565 silencing using a pool of three shRNA in 3 primary MN cells compared to scramble; a representative
566 WB is shown underneath. Data are presented as mean \pm SD; *** = $p \leq 0.001$. **B** Percentage of reduction
567 in *STAT1* expression associated to *STAT1* sh-RNA-mediated silencing compared to control shown in
568 **A**; Data are presented as mean \pm SEM; ** = $p \leq 0.01$. **C-D** Representative images of the
569 immunofluorescent staining of STAT1 (green) and the proliferation marker Ki67 (red) (**D**) after *STAT1*
570 sh-RNA-mediated silencing compared to scramble. Nuclei are stain with DAPI (blue). **E-F** Histogram
571 presenting the statistical reduction of proliferating cells and total number of cells (**F**) after STAT1-KD
572 compared to control. Data are presented as mean \pm SD; *** = $p \leq 0.001$, ** = $p \leq 0.01$. **G** Representative
573 WB, showing the reduction in AKT and ERK1/2 phosphorylation following STAT1 silencing. **H** Histogram
574 representing the WB quantification of total and phosphorylated AKT and ERK1/2 following STAT1
575 silencing in 3 primary MN cells, *** = $p \leq 0.001$, ns= not significant.

576

[NOA-D-19-00065R2](#)

577 **Fig. 4** STAT1 activating mutations induce phosphorylation of AKT, ERK1/2 and an increased
578 proliferation of U251-MG cells. **A** WB representing total and phosphorylated STAT1 levels in U251-MG
579 compared to HMC and BM-1 cells. **B** WB showing overexpression of STAT1-WT and activating mutants
580 in U251-MG cells and the related activation of pAKT and pERK1/2. **C** *STAT1* expression levels in U251-
581 MG cells normalised vs. *STAT1* expression levels in pCDNA transfected cells (~~=1~~). Data are presented
582 as mean \pm SEM; *** = $p \leq 0.001$. **D** Histogram presenting the statistical increased in cell proliferation in
583 U251-MG cells overexpressing the activating STAT1 mutants (STAT1-Y701F, STAT1-S727E, STAT1-
584 Y701F/S727E). Data were normalised for STAT1-pCDNA-transfected cells and presented as FC of
585 growth vs. STAT1-WT; *** = $p \leq 0.001$.

586

[NOA-D-19-00065R2](#)

587 **Fig. 5** The constitutive activation of the EGFR in meningioma induces STAT1 phosphorylation. **A**
588 Representative WB analysis of total and pEGFR-Y1068 in meningioma, when compared to control.
589 Upper panel: WHO I, II and III meningioma tissues compared to NMT; lower panel: BM-1 and primary
590 MN cells compared to HMC. **B** WB of STAT1 and pSTAT1 protein levels after treatment with 5 μ M of
591 canertinib, afatinib and erlotinib in BM-1 cells. The reduced levels pEGFR-Y1068 confirmed drug activity.
592 **C** ATP-proliferation assay performed in BM-1 cells after treatment with different concentrations of
593 canertinib, afatinib and erlotinib for 24 h. **D** WB analysis of STAT1, pSTAT1 and other markers of
594 proliferation in primary MN cells after treatment with 10 μ M of canertinib. **E** Histograms representing
595 WB quantification at 3 and 24 h for STAT1, pSTAT1, pAKT, pERK 1/2 and Cyclin D1 after canertinib
596 treatment in three different primary MN cells (see Supplementary Fig. 4). Data are presented as mean
597 \pm SEM, * = $p < 0.05$; ** = $p < 0.01$; *** = $p < 0.001$. **F** q-PCR analysis showing the statistical reduction of
598 *STAT1* gene expression at 3, 6 and 24 h after treatment with 10 μ M of canertinib (n=3). Data are
599 presented as mean \pm SEM; ** = $p < 0.01$. **G** WB representing STAT1 and pSTAT1 in BM-1 cells, following
600 treatment with EGF (50 ng/ml) for 5, 30 and 60 minutes.

NOA-D-19-00065R2

1 **Constitutive activation of the EGFR-STAT1 axis increases**
2 **proliferation of meningioma tumor cells**

3
4 **Sara Ferluga¹, Daniele Baiz¹, David A. Hilton², Claire L. Adams¹, Emanuela Ercolano¹, Jemma**
5 **Dunn¹, Kayleigh Bassiri¹, Kathreena M. Kurian³ and C. Oliver Hanemann^{1, 4}**

6
7 ¹ University of Plymouth, Faculty of Health: Medicine, Dentistry and Human Sciences, The Institute of
8 Translational and Stratified Medicine, The John Bull Building, Plymouth Science Park, Research Way,
9 Plymouth UK, PL6 8BU

10 ² Cellular and Anatomical Pathology, Plymouth Hospitals NH Trust, Derriford Road, Plymouth UK, PL6
11 8DH

12 ³ Department of Neuropathology, Pathology Sciences, Southmead Hospital, Southmead Road, Bristol
13 UK, BS10 5NB

14 ⁴ **Corresponding author:** Prof. Clemens Oliver Hanemann MD, FRCP, Director of the Institute of
15 Translational and Stratified Medicine, University of Plymouth, Faculty of Health: Medicine, Dentistry and
16 Human Sciences, Plymouth Science Park, Research Way, Plymouth UK, PL6 8BU. Phone: +44
17 1752437418, Fax: +441752517846, E-mail: Oliver.Hanemann@plymouth.ac.uk

18
19 **Running Title:** EGFR-STAT1 tumor-promoting role in meningioma

20
21 **Funding:** This work was funded by Brain Tumour Research. DB was partially funded by the FP7 Marie
22 Curie Actions (PCOFUND-GA-20126001). Tissue samples were obtained from University Hospitals
23 Plymouth as part of the UK Brain Archive Information Network (BRAIN UK) which is funded by the
24 Medical Research Council.

25
26 **Conflict of Interest:** Authors declare that there are no conflicts of interest.

27
28 **Authorship:** Designing and execution of most of the experiments, data interpretation, manuscript and
29 figures preparation – SF

30 Designing and execution of gene expression studies, data interpretation, writing of the related part,
31 performing experimental revisions and addressing comments to reviewers, proofreading of the
32 manuscript – DB

33 Designing and execution of immunohistochemistry, data interpretation, writing of the related part – DAH

34 Designing and execution of the flow cytometry experiments, data interpretation, writing of the related
35 part – CLA

36 Managing of tumor digestions and primary MN cells cultures – EE

37 Supporting with Western blot studies on MN Merlin status – JD

38 Supporting with the initial identification of STAT1 in meningioma – KB

39 Providing the majority of the samples involved in the study – KMK

40 Intellectual input to the critical design of the study, data interpretation, manuscript preparation - COH

41

42 **Total Word Count: 6217**

43

44

45

46

47

48

49 **Abstract**

50 **Background:** Meningiomas are the most frequent primary brain tumors of the central nervous system.
51 The standard of treatment is surgery and radiotherapy, but effective pharmacological options are not
52 available yet. The well-characterised genetic background stratifies these tumors in several subgroups,
53 thus increasing diversification. We identified EGFR-STAT1 overexpression and activation as a common
54 identifier of these tumors.

55 **Methods:** We analysed STAT1 overexpression and phosphorylation in 131 meningiomas of different
56 grades and locations by utilising several techniques, including Western blots, qPCR and
57 immunocytochemistry. We also silenced and overexpressed wild-type and mutant forms of the gene
58 to assess its biological function and its network. Results were further validated by drug testing.

59 **Results:** STAT1 was found widely overexpressed in meningioma but not in the corresponding healthy
60 controls. The protein showed a constitutive phosphorylation not dependent on the JAK/STAT pathway.
61 *STAT1* knock-down resulted in a significant reduction of cellular proliferation and deactivation of AKT
62 and ERK1/2. STAT1 is known to be activated by EGFR, so we investigated the tyrosine kinase and
63 found that EGFR was also constitutively phosphorylated in meningioma and was responsible for the
64 aberrant phosphorylation of STAT1. The pharmaceutical inhibition of EGFR caused a significant
65 reduction in cellular proliferation and of overall levels of Cyclin D1, pAKT and pERK1/2.

66 **Conclusions:** STAT1 EGFR-dependent constitutive phosphorylation is responsible for a positive
67 feedback loop that causes its own overexpression and consequently an increased proliferation of the
68 tumor cells. These findings provide the rationale for further studies aiming to identify effective
69 therapeutic options in meningioma.

70

71

72

73

74 **Keywords:** Meningioma, STAT1, EGFR, cancer, brain

75

76 **Importance of the Study**

77 Meningioma accounts for 37% of primary brain tumors. This year in the United States an estimated
78 thirty-two thousand people will be diagnosed with meningioma. These tumors can cause mild to severe
79 morbidity and even WHO grade I can have a more aggressive clinical course. Therapeutic options are
80 still limited to surgical resection and radiotherapy since more effort is needed to decipher the communal
81 molecular mechanisms that define meningiomas despite their genetic background.

82 Aiming to discover novel therapeutic targets, we identified STAT1 as aberrantly overexpressed and
83 constitutively activated in most of the meningioma examined. Its activation is dependent on the
84 constitutive phosphorylation of EGFR and leads to an increased proliferation of tumor cells. We show
85 that specific EGFR inhibition can reduce tumor cell proliferation and we show evidence why previous
86 trials failed. Therefore, we suggest that this therapeutic strategy be re-evaluated.

87

88

89 Introduction

90 Meningiomas are the most common primary brain tumors, classified meningiomas as Grade I (~80%),
91 atypical Grade II (15-20%) and anaplastic/malignant Grade III (1-3%). Surgery is the primary choice of
92 treatment; complete resection may be curative but it can be achieved only for permissive locations¹.
93 The genetic background of meningioma is well characterised, with inactivation/deletion of *NF2* found in
94 ~60% of sporadic meningiomas².

95 Previously, we identified phosphorylated Signal Transducer and Activator of Transcription 1 (STAT1)
96 as overexpressed in the grade I meningioma cell line³ and phosphorylated STAT1 in meningioma tissue
97 of all grades⁴. In addition, we identified phosphorylation of STAT3 among remaining STAT family
98 members^{3,4}. STAT1 belongs to the STAT protein family that comprise seven members (STAT1-4,
99 STAT5A, STAT5B and STAT6), and it can be phosphorylated on the tyrosine 701 (Y701) and the serine
100 727 (S727)^{5,6}. STATs are essential components of the evolutionarily conserved JAK/STAT signalling
101 pathway^{4,7} that plays a role in immune response^{8,9} and its dysregulation is linked to cancer^{10,11}. This
102 canonical pathway is activated by ligands including interferons, interleukins and some growth factors,
103 binding to their receptors thus inducing phosphorylation of the JAKs (Janus Kinases), leading to
104 tyrosine-STAT phosphorylation by JAKs^{4,6}. In addition STATs can also be phosphorylated by receptor
105 tyrosine kinases and cytoplasmic non-receptor tyrosine kinases⁵. Phosphorylated STATs homo- and
106 hetero-dimerize entering the nucleus to regulate transcription of target genes^{6,12}. JAKs include JAK1-3
107 and TYK2. JAK1 and JAK2 are phosphorylated following type-II interferon (IFN γ) stimulation, while
108 JAK1 and TYK2 are activated in type-I interferon signalling (IFN α , IFN β ; etc.)⁴⁻⁶. Activated JAK/STAT
109 pathway can be quenched by the SOCSs (Suppressors Of Cytokine Signalling), the PIASs (Protein
110 Inhibitors of Activated STAT) and the PTPs (Protein Tyrosine Phosphatases)⁵

111 Activated STAT1 acts as a transcriptional regulator, controlling its own transcription as well as the
112 expression of several IFN-regulated genes (IRGs)^{13,14}. STAT1 was considered a tumor suppressor as
113 its expression correlated with good prognosis in several types of cancer¹⁵⁻¹⁸. However, other studies
114 established a pro-tumorigenic role of STAT1, which correlated with its overexpression and activation¹⁹.
115 Due to its function in sensing and regulating cytokine production, STAT1 exerts a role in promoting an
116 immunosuppressive tumor environment^{19,20}. Hence, the overall role of STAT1 in cancer remains
117 complex suggesting that its function is most likely cancer type-dependent.

118 In the present study, we identified STAT1 as overexpressed and phosphorylated in meningioma
119 compared to normal and we show that its overexpression correlates with an increased proliferation of
120 the tumor cells as well as an activation of AKT and ERK1/2. We demonstrate that STAT1
121 overexpression and phosphorylation is not dependent on the JAK/STAT pathway but it depends on a
122 positive feedback loop caused by the constitutive activation of the Epidermal Growth Factor Receptor
123 (EGFR). The pharmaceutical inhibition of EGFR in meningioma caused the deactivation of STAT1 and
124 other cancer-related pathways, eventually leading to a significant reduction in cellular proliferation.
125 Our findings underline a crucial role of the EGFR and STAT1 signalling in the pathology of meningiomas
126 and point to a therapeutic potential of its inhibition.

127

128 **Materials and Methods**

129 **Meningioma specimens, tumor digestion and primary meningioma cultures**

130 Meningioma specimens were collected following the ethical approvals received a unique MN number
131 (Supplementary Table 1). Normal meningeal tissue (NMT) was purchased from Analytical Biological
132 Service Inc.

133 Primary cells were generated from 36 fresh tumor tissue. Tissue were disaggregated in DMEM with
134 15% FBS, 100 U/ml penicillin/streptomycin and 20 U/ml Collagenase III (Worthington Biochemical Corp)
135 for 2 h at 37 °C; after cells were pelleted at 1000 rpm for 5 min, resuspended and seeded (modified
136 from²¹). MN cells were cultured in DMEM at 37 °C in 5% CO₂. HMC cells (Caltag Medsystems Ltd)
137 were grown in the recommended medium at 37 °C in 5% CO₂. Cells were kept on average 4-5
138 passages.

139 Normal human meningeal cell were purchased from ScienceCell (UK distributor: Caltag Medsystems;
140 Catalog#1400), U251 glioma cells were purchased from ECACC (Cat n.: 09063001), an immortalized
141 grade 1 meningioma cell line BM-1 were (DSMZ; Cat.n.: ACC 599) and authenticated via genomic
142 fingerprinting (Eurofins Genomics Europe Applied Genomics GmbH).

143 **Western blotting, immunofluorescence and immunohistochemistry**

144 Western blots (WB) from 26 frozen tissues and cell cultures were performed as previously described³.
145 All primary antibodies used are listed in Supplementary Table 2. Immunoreactive bands were quantified
146 using Scion Image software and each band was normalized vs. the corresponding GAPDH.

147 Immunofluorescence of 38 paraffin embedded tissue was performed as previously described³. Confocal
148 microscopy was executed using a Leica DMI6000B; Z-stack micrographs were taken using the 40X or

149 63X objectives. Immunofluorescent images for STAT1-silencing studies were taken with the Olympus
150 CKX41 with the 20X objective; images were processed with the QCapture Pro 6.0 software.

151 For immunohistochemistry, paraffin sections (4µm) were processed as described²². Avidin-biotin
152 blocking solution was used with EDTA pretreatment. Sections were incubated with appropriate biotin-
153 labelled secondary antibody and with horseradish peroxidase for detection using Vectashield Elite
154 (Vector Laboratories UK) according to the manufacturer's protocol. As a control, sections were
155 incubated with omission of the primary antibody.

156 Results were reviewed 'blind' to the histological grade by a neuropathologist (DAH). Semiquantitative
157 assessment of the intensity of immunoreactivity was undertaken and scored as follow: 0 none; 1 weak;
158 2 moderate; 3 strong.

159 **RNA isolation and gene expression analysis**

160 Total RNA was extracted from 95 frozen tissues and cells using the Qiazol® reagent (Qiagen UK),
161 following manufacturer's protocol. The quality, integrity and concentration of RNA were established
162 using the NanoDrop ND-2000 (ThermoFisher Scientific UK).

163 Real-Time PCR (qPCR) was conducted using 50 ng/well employing the EXPRESS One-Step SYBR®
164 GreenERTM kit (Invitrogen) on a LightCycler® 480 System (Roche Diagnostics, Switzerland), following
165 manufacturer's protocol (primers annealing temperature= 58 °C). Primers used were: PrimePCR™
166 SYBR® Green Assay STAT1 (BioRad), hGAPDH (2 µM, Invitrogen- Forward: 5'-
167 GAGAAGGCTGGGGCTCATTT-3'; Reverse 5'-AGTGATGGCATGGACTGTGG-3'). Relative gene
168 expression analysis of STAT1 and GAPDH was calculated using the $2^{-\Delta\Delta C_t}$ method²³, employing the
169 HMC as calibrator.

170 **STAT1 silencing and overexpression**

171 Stat1 shRNA Lentiviral Particles (Santa Cruz Biotechnology, sc-44123-V), containing 3 target-specific
172 constructs that encode 19-25nt (plus hairpin) or scramble shRNA control (Santa Cruz Biotechnology,
173 sc-108080), were added onto the cells in media containing protamine sulfate salt (8 µg/ ml) (Sigma).
174 Cells were infected for 48 h before applying puromycin (5 µg/ml) for 3 days.

175 *STAT1-WT* gene was cloned into pCDNA3.1+ in a two-step process using the following primers:
176 STAT1-F1 (5'-AAAGCTAGCGCCCGCCATGTCTCAG-3'), STAT1-R1 (5'-
177 CGTCTCGAGGTCAATTACCAAACCAGGCT-3') for the first part; STAT1-2F (5'-
178 GACCTCGAGACGACCTCTCT), STAT1-2R (5'-AGTGTTTAACTTAATTAATACTACTGTGTTCA-3')
179 for the second part. The 551 bp long STAT1 part in between the restriction sites HindIII and EcoRI was
180 synthesised (GeneArt, ThermoFisher Scientific) to generate the following mutations: Y701F, S727E and

181 Y701F/S727E; each one was cloned into pCDNA-STAT1-WT to replace the wild-type part. All
182 generated plasmids were sequenced before further use (Eurofins). U251-MG cells were transfected
183 and selected as previously described ²⁴.

184 **Ki-67 staining and Proliferation assay**

185 For Ki-67 staining, cells were grown on chamber slides, lentivirus-transfected and stained as previously
186 described³.

187 For U251-MG proliferation assay, the pool of U251-MG selected cells, transfected with pCDNA, STAT1-
188 WT and the three mutants, were seeded at 1000 cell/well in 96 well plates and proliferation was
189 determined after 24, 48 and 72 h using the 'CellTiter-Glo® Luminescent Cell Viability Assay' as
190 recommended by the supplier (Promega).

191 For drug testing, meningioma cells (~3000 cell/well) were plated in 96-well culture plates and allowed
192 to proliferate for 24 h. Cell proliferation was calculated as percentage of control cells. Graphs were
193 generated using GraphPad Prism 5.

194 **Flow cytometry analysis**

195 Confluent meningioma cells were resuspended in ice-cold staining buffer (PBS, 2%FBS) at a final
196 concentration of 1×10^5 cells. Cells were stained for 30 min at RT in the dark with the following: CD45-
197 FITC, HLA-DR-PE, CD14-PerCP5.5 and CD44 –APC (Becton Dickinson Biosciences, Pharmigen),
198 washed twice with 2 ml of staining buffer and centrifuged at 1500 rpm for 5 min at 4°C . The relevant
199 single isotype controls were used. Data acquisition was collected on 1×10^4 cells on a Accuri flow
200 cytometer (BD Biosciences) and analysis was performed using the Flow Jo software v10.0 (FlowJo
201 LLC, Ashland, OR).

202 **Statistical analysis**

203 Probability (p) values were calculated using the Student's t-Test or the ANOVA one-way analysis of
204 variance, using GraphPad Prism 5.01 and MS Excel 2016 software. P values <0.05 were considered
205 statistically significant. The results are expressed as means \pm SD or \pm SEM.

206

207

208

209

210

211 **Results**

212 **STAT1 is overexpressed and aberrantly activated in meningioma**

213

214 We analysed STAT1 expression in meningioma tumors compared to normal meninges (NMT). In all
215 cases STAT1 was overexpressed and in most of the cases, we detected high levels of phosphorylated
216 STAT1 (Y701 and S727) (representative Western blot of Fig. 1A and qPCR of Fig. 1C).
217 Immunohistochemical studies validated STAT1 overexpression in all meningioma samples (Fig. 1B);
218 also pSTAT1-Y701 and -S727 showed higher staining compared to normal meninges and an increasing
219 score throughout the grades. As control, we further analysed STAT1 and pSTAT1 abundance in two
220 additional normal meninges and a normal brain (Fig. 1D).

221 Then, we examined STAT1 expression and phosphorylation in meningioma-derived primary cells (MN)
222 and in BM-1²⁵ compared to HMC. MN cells were used between passage 3 and 5 and no B/T
223 lymphocytes or infiltrating macrophages were detected (Supplementary Fig. 1A). All cells were
224 vimentin-positive²⁶ and CD90-negative, suggesting no fibroblasts contamination²⁷ (Supplementary Fig.
225 1B). STAT1 was found overexpressed in BM-1 and MNs compared to HMC and both pSTAT1-Y701
226 and -S727 were present across all samples while faint and undetectable in HMC (Fig. 1C). Q-PCR
227 analysis confirmed that *STAT1* expression was higher in most of the MNs and in BM-1 compared to
228 control (Fig. 1F). Of note, STAT1 overexpression was independent of Merlin status (Supplementary Fig.
229 1C, D).

230 Furthermore, pSTAT1-Y701 showed a cytoplasmic localization while pSTAT1-S727 was nuclear (Fig.
231 1B), in agreement with the immunofluorescent staining of primary MN cells (Fig. 1G).

232 Overall, we examined 131 meningiomas vs. 10 normal meninges and 5 normal brains and we
233 demonstrate substantial overexpression of STAT1 in 100 of them with a variety of methods
234 (Supplementary Table 1).

235

236 **STAT1 constitutive phosphorylation is not dependent on the JAK/STAT pathway**

237 To further investigate STAT1 phosphorylation in the context of the tumor environment, we examined
238 meningioma tumor lysates for the presence of interferon gamma (IFN γ) and tumor-associated
239 macrophages by using CD163 marker staining preferentially M2 macrophages²⁸. Variable protein

240 levels of IFN γ and CD163 were detected, but there was no evident correlation with STAT1
241 phosphorylation and no JAK1 phosphorylation was detected (Fig 2A).

242 STAT1 usually becomes phosphorylated as a result of JAK/STAT pathway activation in response to
243 external stimuli⁶. We examined whether STAT1 overexpression and phosphorylation was dependent
244 on the culture conditions and secreted factors. Culturing HMC in serum-free (SF) media and in BM-1
245 conditioned media, and BM-1 in SF media, we confirmed that STAT1 overexpression and
246 phosphorylation was not due to external factors, but most likely to an intrinsic activation (Fig. 2B).

247

248 Next, we decided to test the ability of the JAK/STAT pathway to respond to activating stimuli in
249 meningioma cells. HMC and two MNs were treated with IFN γ ; in HMC, JAK1 and JAK2 activated within
250 10 min after treatment as well as pSTAT1-Y701 whilst pSTAT1-S727 phosphorylated within 1 h. The
251 same behaviour was observed in MNs confirming that the JAK/STAT pathway was functional; however,
252 STAT1 was constitutively phosphorylated in non-treated cells while pJAK1 and pJAK2 were not (Fig.
253 2C). The same experiment, performed using interferon alpha (IFN α), produced comparable results
254 (Supplementary Fig. 2A).

255 After activation, pSTAT1 is known to dimerize and translocate into the nucleus⁶. IFN γ treatment was
256 indeed able to induce pSTAT1-Y701 nuclear internalization (Fig. 2D, Supplementary Fig. 2B). Thus,
257 the JAK/STAT1 pathway can be activated *via* IFN in meningioma cells but there was also an IFN-
258 independent intrinsic activation.

259 STAT1 constitutive phosphorylations could be due to a deficient deactivation of the pathway^{4,5,29}. Thus,
260 we analysed the levels of the SOCSs and the PIASs in HMC, BM-1 and MN cells (Fig. 2E), which did
261 not correlate with the constitutive phosphorylation of STAT1 observed in these samples (Fig. 1E).

262 Overall, these data suggest that the JAK/STAT pathway is functional but not over-activated. Therefore,
263 we hypothesized other mechanisms must be involved in maintaining STAT1 in a constitutive
264 phosphorylated form in the meningioma samples analyzed.

265

266 **STAT1 overexpression is associated with an increased proliferation of meningioma cells**

267 To investigate the biological significance of STAT1 overexpression in meningioma we silenced the
268 protein in MN cells. Lentiviral-mediated shRNA delivery into the cells produced an over 70% reduction
269 in protein expression (Fig. 3A) and a 50% reduction in gene expression levels compared to scramble
270 (Fig. 3B). STAT1-silenced cells displayed a reduction in STAT1 immunofluorescent staining as well as

271 a reduction in Ki67-positive cells (Fig. 3C). Proliferating cells were reduced from ~22% to less than 5%
272 in MNs (Fig. 3D, E). This was in agreement with the reduction of the total number of cells (Fig. 3F) and
273 a 40% reduction of Cyclin D1 (Fig. 3A). A similar effect was observed in BM-1 cells (Supplementary Fig.
274 3A-D). Taken together, our results demonstrate that STAT1 overexpression is associated to an
275 increased proliferation of meningioma tumor cells.

276 The MAPK-ERK and the AKT pathways are known to be active in meningioma and to influence tumor
277 progression³⁰. After STAT1-KD, both AKT and ERK1/2 showed a 95% and 80% reduction in protein
278 phosphorylation respectively (Fig. 3G, H), supporting a critical involvement of STAT1 in the activation
279 of pro-proliferative pathways.

280

281 **Phosphorylated STAT1 affects activation of AKT and ERK1/2 and cellular proliferation**

282 We used phosphomimetics to further characterise the effects of STAT1 phosphorylation. Phenylalanine
283 (F) and Glutamic acid (E) are used to mimic the structure of a phosphorylated tyrosine (Y) and
284 phosphorylated serine (S) respectively³¹. We produced three different STAT1 mutants: Y701F, S727E
285 and the double mutant Y701F/S727E. Since STAT1 is constitutively phosphorylated in meningioma, we
286 used U251-MG cells as a model because this cell line showed levels of total and pSTAT1 lower than
287 HMC (Fig. 4A). STAT1 overexpression in U251-MG for wild-type (WT) and mutants was confirmed by
288 WB and qPCR (Fig. 4B, C). STAT1 overexpression in U251-MG cells determined an increased
289 phosphorylation of AKT and ERK1/2, where the effect was particularly evident for pERK1/2 in STAT1-
290 S727E and STAT1-Y701F/S727E mutants (Fig. 4B).

291 The proliferation of transfected cells was measured over a period of 72 h and normalised for the empty-
292 vector control. All STAT1 mutants showed a significantly increased proliferation rate compared to
293 STAT1-WT; interestingly, the double mutant STAT1- Y701F/S727E, which represents STAT1 in its
294 maximal activated condition, determined the highest pro-proliferative effect in U251-MG cells (Fig. 4B,
295 4D).

296 These experiments confirmed that the constitutive phosphorylation of STAT1 on both phosphosites
297 affects the activation of the AKT and ERK1/2 pathways as well as the proliferation of the cells in
298 agreement with STAT1 knock-down results in meningioma.

299

300 **EGFR constitutive phosphorylation is responsible for STAT1 overexpression and activation**

301 It has been previously shown that STAT1 can be phosphorylated by EGFR, a key tyrosine kinase
302 relevant to the majority of tumors^{32,33}. We examined the EGFR status in meningioma tissues and cells,

303 detecting high levels of pEGFR in both tumor lysates and meningioma cells, when compared to normal
304 meningeal tissue (NMT) and HMC (Fig. 5A).

305 To test whether the constitutive phosphorylation of EGFR was responsible for STAT1 phosphorylation,
306 we treated BM-1 cells with three different EGFR inhibitors (canertinib andafatinib, 2nd generation
307 irreversible inhibitors) and erlotinib (1st generation, reversible inhibitor), , for 30 min, 3, 6 and 24 h³⁴.
308 Canertinib (and similarly afatinib) decreased STAT1 expression of about 60% within 24 h upon;
309 pSTAT1-Y701 was almost abolished 30 min after treatment but was restored at 24 h while pSTAT1-
310 S727 showed a decrease of about 90% compared to vehicle at 24 h (Fig. 5B). Almost no effect on total
311 and pSTAT1 was detected after treatment with erlotinib, which did not cause an evident decrease in
312 pEGFR-Y1068 after treatment (Fig. 5B).

313 EGFR blockade *via* canertinib and afatinib decreased pSTAT1 levels and determined a concentration-
314 dependent decrease of cellular proliferation already at 24 h after treatment (Fig. 5C), with erlotinib being
315 ineffective.

316 Since canertinib showed the strongest effect on STAT1 in BM-1 cells, we tested its effects on primary
317 MNs (Fig. 5D). Canertinib was active in reducing EGFR constitutive phosphorylation in MN cells,
318 reducing p-STAT1 levels after canertinib treatment; pSTAT1-S727 reduced of 65% already 3 h after
319 treatment and stayed low over the 24 h; phosphorylated STAT1-Y701 also showed about 50% reduction
320 3 h after treatment and recovered between 6 and 24 h (Fig. 5D, E Supplementary Fig. 4).

321 Phospho-AKT and pERK1/2 showed a decrease of about 70% and Cyclin D1 reduced to 50% in 24 h
322 (Fig. 5D,E,Supplementary Fig. 4).

323 We wanted to examine whether the inhibition of pEGFR and thus of pSTAT1 had any effect on *STAT1*
324 expression, as STAT1 is known to regulate its own transcription³⁵. *STAT1* expression levels reduced
325 by ~50% 24 h after treatment with canertinib in MNs (Fig. 5F), consistently with a 30% reduction in
326 protein level observed by WB analysis (Fig. 5D, E, Supplementary Fig. 4).

327 Lastly, to confirm the link between EGFR activation and STAT1 phosphorylation, we treated BM-1 cells
328 with the Epidermal Growth Factor (EGF) for 5, 30 and 60 minutes. Upon EGF treatment STAT1 was
329 phosphorylated on Y701 within 5 minutes and on S727 within 30 minutes (Fig. 5G).

330 Hence, we showed that EGFR is responsible for STAT1 overexpression and constitutive activation in
331 meningioma, which consequently increases proliferation of the tumor cells.

332

333

334

335

336

337

338 Discussion

339 Meningiomas are the most common primary brain tumor but there are no therapeutic options available
340 other than surgery and radiotherapy^{1,36}. The well-defined genetic background of meningioma is leading
341 towards an increasing stratification of these tumors into subtypes^{37,38}; however, common features
342 should still be investigated.

343 We identified STAT1 as overexpressed and activated in 84% of meningioma examined. The only
344 study exploring the expression levels of STAT and JAK superfamilies in meningiomas was published
345 in 1999 showing higher immunoreactivity of JAK1 (see also Supplementary Fig. 2C), JAK2 and the
346 STATs in meningiomas compared to normal dura³⁹. Our data confirmed the expression of the JAKs in
347 MN cells and in HMC; we showed that the JAK/STAT pathway is activated by IFN α and IFN γ , inducing
348 nuclear localization of pSTAT1 as seen before³⁹. [As previously reported⁴⁰, activation of STAT1
349 after IFN \$\gamma\$ stimulation occurs via JAK kinases by phosphorylation on Y701, resulting in
350 pSTAT1 translocation into the nucleus and subsequent phosphorylation at S727⁴¹. Double
351 phosphorylation is required for maximal STAT1 activity.](#) However, we show that STAT1 is
352 constitutively phosphorylated in MNs but not in HMC, even without IFN stimulation and in serum-free
353 conditions. In tumor lysates, STAT1 phosphorylation was not consistent with the presence of M2-
354 polarised macrophages or IFN γ suggesting that the constitutive activation of STAT1 was not related to
355 the JAK/STAT pathway.

356 To better understand the meaning of this STAT1 phosphorylation we used phosphomimetics,
357 generating STAT1-Y701F, STAT1-S727E and STAT1-Y701F/S727E mutants. The overexpression of
358 these mutants induced activation of two central nodes in cancer signalling, AKT and ERK1/2, and
359 increased cellular proliferation. A similar approach was used on STAT3 in human prostate cancer cell,
360 where the mutant STAT3-Y705F/S727E promoted survival, growth and invasion. They showed that the
361 mutation S727E was increasing the transcription of c-Myc, which is an essential activator of cell growth

362 and proliferation³¹. It is very likely that a similar mechanism is happening also in meningioma, where
363 STAT1-S727 showed a predominant nuclear localization exerting its role of transcriptional regulator.
364 We also showed the link between STAT1 overexpression and the increased proliferation of the tumor
365 cells. This effect is most likely linked to an activating cascade involving ERK1/2 and AKT, since their
366 activated state and cell proliferation were almost aborted after STAT1 silencing. The activation of the
367 MAPK pathway is involved in both proliferation and apoptosis in meningioma³⁰, and we recently
368 published a proteomic profiling of meningioma, identifying the aberrant activation of the PI3K/AKT
369 pathway across all meningioma grades⁴.

370 Aiming to identify the kinase responsible for STAT1 activation, we examined the status of EGFR, a
371 tyrosine kinase able to phosphorylate STAT1^{33,42,43}. EGFR was overexpressed and constitutively
372 phosphorylated on Y1068 in all of the MN cells examined but not in HMC. To test whether EGFR
373 phosphorylation was responsible for the constitutive activation of STAT1 we used three specific EGFR
374 inhibitors canertinib, afatinib and erlotinib⁴⁴. Whilst canertinib and afatinib, had a similar effect in
375 reducing STAT1 phosphorylation on both phosphosites as well as on cell proliferation and viability,
376 erlotinib, did not produce any significant effect. Interestingly this result is consistent with the
377 unsuccessful clinical trial of erlotinib on recurrent meningiomas⁴⁵. Erlotinib is a first generation ATP
378 dependent reversible rather broad inhibitor⁴⁶, Afinitinib and Canertinib are non reversible second
379 generation with high pEC50 <https://www.proteomicsdb.org/#analytics/selectivity>

380 In MN cells, canertinib (and afatinib) caused the de-phosphorylation of STAT1-Y701 and S&27 within
381 6and 24H respectively. Similarly, EGF stimulation induces an immediate and direct phosphorylation on
382 Y701 and a later one on S727, suggesting the activation of an additional kinase downstream of EGFR,
383 which is probably part of the MAPK/ERK1/2 pathway⁴⁷. Indeed previous studies in pancreatic cancer
384 demonstrated the relationship between EGFR and the downstream signalling regulators like pAKT,
385 pERK1/2 and Cyclin D1³³. In agreement, after canertinib treatment and after STAT1 silencing, we
386 observed a significant reduction of pAKT and pERK1/2. Overall, levels of Cyclin D1 also displayed a
387 significant reduction, consistently with the reduction in proliferation observed after STAT1 silencing and
388 canertinib treatment.

389 The observed reduction in STAT1 expression suggest a feedback regulatory mechanism of pSTAT1 on
390 its own promoter, already documented³⁵, as well as an EGFR/HER2-dependent regulation as previously
391 shown in glioblastoma and breast cancer cell lines⁴⁸.

392 In conclusion, we provide clear evidence of STAT1 overexpression in meningioma of different genotype
393 and its correlation with an increased cellular proliferation. We demonstrate that STAT1 is aberrantly

394 phosphorylated on both phosphosites, not because of the JAK/STAT pathway activation but because
395 of the constitutive phosphorylation of EGFR, which elicits activation of the MAPK/ERK and PI3K/AKT
396 pathways and an increase in the overall levels of Cyclin D1 and STAT1. Although the whole mechanism
397 should be additionally studied to give a thorough understanding of the activating cascade and all the
398 partners involved in it, our studies set the basis for re-evaluating EGFR inhibition in meningioma as
399 possible therapeutic option.

400 **References**

- 401 1. Whittle IR, Smith C, Navoo P, Collie D. Meningiomas. *Lancet*. 2004; 363(9420):1535-
402 1543.
- 403 2. Suppiah S, Nassiri F, Bi WL, et al. Molecular and translational advances in
404 meningiomas. *Neuro Oncol*. 2019; 21(Supplement_1):i4-i17.
- 405 3. Bassiri K, Ferluga S, Sharma V, et al. Global Proteome and Phospho-proteome
406 Analysis of Merlin-deficient Meningioma and Schwannoma Identifies PDLIM2 as a
407 Novel Therapeutic Target. *EBioMedicine*. 2017; 16:76-86.
- 408 4. Dunn J, Ferluga S, Sharma V, et al. Proteomic analysis discovers the differential
409 expression of novel proteins and phosphoproteins in meningioma including NEK9,
410 HK2 and SET and deregulation of RNA metabolism. *EBioMedicine*. 2018.
- 411 5. Lee M, Rhee I. Cytokine Signaling in Tumor Progression. *Immune Netw*. 2017;
412 17(4):214-227.
- 413 6. Kiu H, Nicholson SE. Biology and significance of the JAK/STAT signalling pathways.
414 *Growth Factors*. 2012; 30(2):88-106.
- 415 7. O'Shea JJ, Schwartz DM, Villarino AV, Gadina M, McInnes IB, Laurence A. The JAK-
416 STAT pathway: impact on human disease and therapeutic intervention. *Annu Rev*
417 *Med*. 2015; 66:311-328.
- 418 8. van de Veerdonk FL, Plantinga TS, Hoischen A, et al. STAT1 mutations in autosomal
419 dominant chronic mucocutaneous candidiasis. *N Engl J Med*. 2011; 365(1):54-61.
- 420 9. Holland SM, DeLeo FR, Elloumi HZ, et al. STAT3 mutations in the hyper-IgE
421 syndrome. *N Engl J Med*. 2007; 357(16):1608-1619.
- 422 10. You Z, Xu D, Ji J, Guo W, Zhu W, He J. JAK/STAT signal pathway activation
423 promotes progression and survival of human oesophageal squamous cell carcinoma.
424 *Clin Transl Oncol*. 2012; 14(2):143-149.
- 425 11. Tu Y, Zhong Y, Fu J, et al. Activation of JAK/STAT signal pathway predicts poor
426 prognosis of patients with gliomas. *Med Oncol*. 2011; 28(1):15-23.
- 427 12. Lillemeier BF, Koster M, Kerr IM. STAT1 from the cell membrane to the DNA. *EMBO*
428 *J*. 2001; 20(10):2508-2517.
- 429 13. Kohanbash G, Okada H. MicroRNAs and STAT interplay. *Semin Cancer Biol*. 2012;
430 22(1):70-75.
- 431 14. Ramana CV, Chatterjee-Kishore M, Nguyen H, Stark GR. Complex roles of Stat1 in
432 regulating gene expression. *Oncogene*. 2000; 19(21):2619-2627.
- 433 15. Simpson JA, Al-Attar A, Watson NF, Scholefield JH, Ilyas M, Durrant LG.
434 Intratumoral T cell infiltration, MHC class I and STAT1 as biomarkers of good
435 prognosis in colorectal cancer. *Gut*. 2010; 59(7):926-933.
- 436 16. Chen G, Wang H, Xie S, Ma J, Wang G. STAT1 negatively regulates hepatocellular
437 carcinoma cell proliferation. *Oncol Rep*. 2013; 29(6):2303-2310.
- 438 17. Sun Y, Yang S, Sun N, Chen J. Differential expression of STAT1 and p21 proteins
439 predicts pancreatic cancer progression and prognosis. *Pancreas*. 2014; 43(4):619-
440 623.
- 441 18. Schneckleithner C, Bago-Horvath Z, Dolznig H, et al. Putting the brakes on
442 mammary tumorigenesis: loss of STAT1 predisposes to intraepithelial neoplasias.
443 *Oncotarget*. 2011; 2(12):1043-1054.
- 444 19. Meissl K, Macho-Maschler S, Muller M, Strobl B. The good and the bad faces of
445 STAT1 in solid tumours. *Cytokine*. 2017; 89:12-20.
- 446 20. Hix LM, Karavitis J, Khan MW, Shi YH, Khazaie K, Zhang M. Tumor STAT1
447 transcription factor activity enhances breast tumor growth and immune suppression
448 mediated by myeloid-derived suppressor cells. *J Biol Chem*. 2013; 288(17):11676-
449 11688.
- 450 21. James MF, Lelke JM, Maccollin M, et al. Modeling NF2 with human arachnoidal and
451 meningioma cell culture systems: NF2 silencing reflects the benign character of
452 tumor growth. *Neurobiol Dis*. 2008; 29(2):278-292.
- 453 22. Hilton DA, Ristic N, Hanemann CO. Activation of ERK, AKT and JNK signalling
454 pathways in human schwannomas in situ. *Histopathology*. 2009; 55(6):744-749.

- 455 **23.** Livak KJ, Schmittgen TD. Analysis of relative gene expression data using real-time
456 quantitative PCR and the 2(-Delta Delta C(T)) Method. *Methods*. 2001; 25(4):402-
457 408.
- 458 **24.** Ferluga S, Hantgan R, Goldgur Y, Himanen JP, Nikolov DB, Debinski W. Biological
459 and structural characterization of glycosylation on ephrin-A1, a preferred ligand for
460 EphA2 receptor tyrosine kinase. *J Biol Chem*. 2013; 288(25):18448-18457.
- 461 **25.** Puttmann S, Senner V, Braune S, et al. Establishment of a benign meningioma cell
462 line by hTERT-mediated immortalization. *Lab Invest*. 2005; 85(9):1163-1171.
- 463 **26.** Schwechheimer K, Kartenbeck J, Moll R, Franke WW. Vimentin filament-desmosome
464 cytoskeleton of diverse types of human meningiomas. A distinctive diagnostic
465 feature. *Lab Invest*. 1984; 51(5):584-591.
- 466 **27.** Sorrell JM, Caplan AI. Fibroblasts-a diverse population at the center of it all. *Int Rev*
467 *Cell Mol Biol*. 2009; 276:161-214.
- 468 **28.** Komohara Y, Horlad H, Ohnishi K, et al. M2 macrophage/microglial cells induce
469 activation of Stat3 in primary central nervous system lymphoma. *J Clin Exp Hematop*.
470 2011; 51(2):93-99.
- 471 **29.** Seif F, Khoshmirsafa M, Aazami H, Mohsenzadegan M, Sedighi G, Bahar M. The
472 role of JAK-STAT signaling pathway and its regulators in the fate of T helper cells.
473 *Cell Commun Signal*. 2017; 15(1):23.
- 474 **30.** Mawrin C, Sasse T, Kirches E, et al. Different activation of mitogen-activated protein
475 kinase and Akt signaling is associated with aggressive phenotype of human
476 meningiomas. *Clin Cancer Res*. 2005; 11(11):4074-4082.
- 477 **31.** Qin HR, Kim HJ, Kim JY, et al. Activation of signal transducer and activator of
478 transcription 3 through a phosphomimetic serine 727 promotes prostate
479 tumorigenesis independent of tyrosine 705 phosphorylation. *Cancer Res*. 2008;
480 68(19):7736-7741.
- 481 **32.** Tong J, Taylor P, Moran MF. Proteomic analysis of the epidermal growth factor
482 receptor (EGFR) interactome and post-translational modifications associated with
483 receptor endocytosis in response to EGF and stress. *Mol Cell Proteomics*. 2014;
484 13(7):1644-1658.
- 485 **33.** Seshacharyulu P, Ponnusamy MP, Rachagani S, et al. Targeting EGF-receptor(s) -
486 STAT1 axis attenuates tumor growth and metastasis through downregulation of
487 MUC4 mucin in human pancreatic cancer. *Oncotarget*. 2015; 6(7):5164-5181.
- 488 **34.** Roskoski R, Jr. ErbB/HER protein-tyrosine kinases: Structures and small molecule
489 inhibitors. *Pharmacol Res*. 2014; 87:42-59.
- 490 **35.** Yang J, Stark GR. Roles of unphosphorylated STATs in signaling. *Cell Res*. 2008;
491 18(4):443-451.
- 492 **36.** Moazzam AA, Wagle N, Zada G. Recent developments in chemotherapy for
493 meningiomas: a review. *Neurosurg Focus*. 2013; 35(6):E18.
- 494 **37.** Brastianos PK, Horowitz PM, Santagata S, et al. Genomic sequencing of
495 meningiomas identifies oncogenic SMO and AKT1 mutations. *Nat Genet*. 2013;
496 45(3):285-289.
- 497 **38.** Clark VE, Harmanci AS, Bai H, et al. Recurrent somatic mutations in POLR2A define
498 a distinct subset of meningiomas. *Nat Genet*. 2016; 48(10):1253-1259.
- 499 **39.** Magrassi L, De-Fraja C, Conti L, et al. Expression of the JAK and STAT
500 superfamilies in human meningiomas. *J Neurosurg*. 1999; 91(3):440-446.
- 501 **40.** Khodarev NN, Roizman B, Weichselbaum RR. Molecular pathways: interferon/stat1
502 pathway: role in the tumor resistance to genotoxic stress and aggressive growth. *Clin*
503 *Cancer Res*. 2012; 18(11):3015-3021.
- 504 **41.** Sadzak I, Schiff M, Gattermeier I, et al. Recruitment of Stat1 to chromatin is required
505 for interferon-induced serine phosphorylation of Stat1 transactivation domain. *Proc*
506 *Natl Acad Sci U S A*. 2008; 105(26):8944-8949.
- 507 **42.** Petschnigg J, Groisman B, Kotlyar M, et al. The mammalian-membrane two-hybrid
508 assay (MaMTH) for probing membrane-protein interactions in human cells. *Nat*
509 *Methods*. 2014; 11(5):585-592.
- 510 **43.** Collins-McMillen D, Stevenson EV, Kim JH, et al. HCMV utilizes a non-traditional
511 STAT1 activation cascade via signaling through EGFR and integrins to efficiently

- 512 promote the motility, differentiation, and polarization of infected monocytes. *J Virol.*
513 2017.
- 514 **44.** Smail JB, Rewcastle GW, Loo JA, et al. Tyrosine kinase inhibitors. 17. Irreversible
515 inhibitors of the epidermal growth factor receptor: 4-(phenylamino)quinazoline- and 4-
516 (phenylamino)pyrido[3,2-d]pyrimidine-6-acrylamides bearing additional solubilizing
517 functions. *J Med Chem.* 2000; 43(7):1380-1397.
- 518 **45.** Norden AD, Raizer JJ, Abrey LE, et al. Phase II trials of erlotinib or gefitinib in
519 patients with recurrent meningioma. *J Neurooncol.* 2010; 96(2):211-217.
- 520 **46.** Conradt L, Godl K, Schaab C, et al. Disclosure of erlotinib as a multikinase inhibitor
521 in pancreatic ductal adenocarcinoma. *Neoplasia.* 2011; 13(11):1026-1034.
- 522 **47.** Vanhatupa S, Ungureanu D, Paakkunainen M, Silvennoinen O. MAPK-induced
523 Ser727 phosphorylation promotes SUMOylation of STAT1. *Biochem J.* 2008;
524 409(1):179-185.
- 525 **48.** Han W, Carpenter RL, Cao X, Lo HW. STAT1 gene expression is enhanced by
526 nuclear EGFR and HER2 via cooperation with STAT3. *Mol Carcinog.* 2013;
527 52(12):959-969.
- 528

529 **Figure Legends**

530

531 **Fig. 1** STAT1 and its phosphorylated forms are overexpressed in meningioma. **A** Representative WB
532 analysis showing the expression of total and pSTAT1 in different grade meningiomas vs. NMT **B**
533 Representative images showing the IHC staining of STAT1 and pSTAT1 in the three grades
534 meningiomas compared to normal meninges (see black arrows) at 200X magnification. Mean scores
535 are presented in the table below for the specimens and the normal controls examined (see also
536 Supplementary Table 1 for the full list of specimens examined and the corresponding scores – n=47).
537 **C** *STAT1* expression levels in WHO I (n=40), WHO II (n=25) and WHO III (n= 10) meningioma tumors
538 normalised vs. normal meningeal tissue (NMT). Data are presented as mean \pm SEM; * = $p \leq 0.05$. **D**
539 WB showing pSTAT1 and STAT1 in normal brain (NB) and additional normal meninges (NMT-1 and
540 NMT-2) compared to sample J6 (meningioma) as positive control. **E** Representative WB analysis of
541 STAT1 and pSTAT1 in BM-1 and in WHO I MN cells (MNs) vs. HMC. **F** *STAT1* expression levels in
542 BM-1 (n=4) and in MN cells (n=24) normalised vs. HMC. Data are presented as mean \pm SEM; ** = $p \leq$
543 0.01. **E G** Confocal z-stack images showing the immunofluorescent staining of STAT1 (red) and
544 pSTAT1 (Y701- green and S727- red) in MN cells vs. HMC. Scale bar 50 μ m. Nuclei were stained with
545 DAPI (blue).

546 **Fig. 2** STAT1 phosphorylation in meningioma cells is not dependent on the JAK/STAT pathway. **A** WB
547 of WHO I meningioma tumor tissue lysates (n=8); the presence of gamma interferon (IFN γ) and
548 macrophage infiltration (CD163) into the tumor were analysed in relation to STAT1 and pSTAT1 levels.
549 Phospho-JAK1 was used to detect activation of the JAK-STAT pathway (*=positive control for pJAK1
550 antibody. **B**). WB of total and pSTAT1 in BM-1 and HMC cells, grown in different culture condition. HMC:
551 HMC cells media; MN: MN cells media; MN-SF: MN-serum free media; MN-SF+FBS: MN serum free
552 for 24 h + FBS for 24h; MN Cond: meningioma cells-conditioned media **C** WB analysis of STAT1 and
553 pSTAT1 protein levels in HMC and two primary MN cells after IFN γ treatment at the concentration of 50
554 ng/ml for the indicated amount of time. Phospho-JAK1 and pJAK2 are shown to confirm the activation of
555 the JAK/STAT pathway. **D** Representative confocal images (z-stack) showing localization of pSTAT1-
556 Y701 (green) and pSTAT1-S727 (red) in primary MN cells before and after IFN γ stimulation (50 ng/ml
557 for 1 h). Scale bar 50 μ m. Nuclei were stain with DAPI (blue). **E** WB analysis of SOCSs and PIASs
558 protein levels in BM-1 and primary MNs compared to HMC.

559 **Fig. 3** STAT1 overexpression increases meningioma cells proliferation. **A** Histogram representing the
560 percentage of statistical reduction in STAT1 and Cyclin D1 protein levels after *STAT1* sh-RNA-mediated
561 silencing using a pool of three shRNA in 3 primary MN cells compared to scramble; a representative
562 WB is shown underneath. Data are presented as mean \pm SD; *** = $p \leq 0.001$. **B** Percentage of reduction
563 in *STAT1* expression associated to *STAT1* sh-RNA-mediated silencing compared to control shown in
564 **A**; Data are presented as mean \pm SEM; **= $p \leq 0.01$. **C-D** Representative images of the
565 immunofluorescent staining of STAT1 (green) and the proliferation marker Ki67 (red) (**D**) after *STAT1*
566 sh-RNA-mediated silencing compared to scramble. Nuclei are stain with DAPI (blue). **E-F** Histogram
567 presenting the statistical reduction of proliferating cells and total number of cells (**F**) after STAT1-KD
568 compared to control. Data are presented as mean \pm SD; *** = $p \leq 0.001$, ** = $p \leq 0.01$. **G** Representative
569 WB, showing the reduction in AKT and ERK1/2 phosphorylation following STAT1 silencing. **H** Histogram
570 representing the WB quantification of total and phosphorylated AKT and ERK1/2 following STAT1
571 silencing in 3 primary MN cells, *** = $p \leq 0.001$, ns= not significant.

572

573 **Fig. 4** STAT1 activating mutations induce phosphorylation of AKT, ERK1/2 and an increased
574 proliferation of U251-MG cells. **A** WB representing total and phosphorylated STAT1 levels in U251-MG
575 compared to HMC and BM-1 cells. **B** WB showing overexpression of STAT1-WT and activating mutants
576 in U251-MG cells and the related activation of pAKT and pERK1/2. **C** *STAT1* expression levels in U251-
577 MG cells normalised vs. *STAT1* expression levels in pCDNA transfected cells. Data are presented as
578 mean \pm SEM; *** = $p \leq 0.001$. **D** Histogram presenting the statistical increased in cell proliferation in
579 U251-MG cells overexpressing the activating STAT1 mutants (STAT1-Y701F, STAT1-S727E, STAT1-
580 Y701F/S727E). Data were normalised for STAT1-pCDNA-transfected cells and presented as FC of
581 growth vs. STAT1-WT; *** = $p \leq 0.001$.

582

583 **Fig. 5** The constitutive activation of the EGFR in meningioma induces STAT1 phosphorylation. **A**
584 Representative WB analysis of total and pEGFR-Y1068 in meningioma, when compared to control.
585 Upper panel: WHO I, II and III meningioma tissues compared to NMT; lower panel: BM-1 and primary
586 MN cells compared to HMC. **B** WB of STAT1 and pSTAT1 protein levels after treatment with 5 μ M of
587 canertininb, afatinib and erlotinib in BM-1 cells. The reduced levels pEGFR-Y1068 confirmed drug activity.
588 **C** ATP-proliferation assay performed in BM-1 cells after treatment with different concentrations of
589 canertininb, afatinib and erlotinib for 24 h. **D** WB analysis of STAT1, pSTAT1 and other markers of
590 proliferation in primary MN cells after treatment with 10 μ M of canertininb. **E** Histograms representing
591 WB quantification at 3 and 24 h for STAT1, pSTAT1, pAKT, pERK 1/2 and Cyclin D1 after canertininb
592 treatment in three different primary MN cells (see Supplementary Fig. 4). Data are presented as mean
593 \pm SEM, * = $p < 0.05$; ** = $p < 0.01$; *** = $p < 0.001$. **F** q-PCR analysis showing the statistical reduction of
594 *STAT1* gene expression at 3, 6 and 24 h after treatment with 10 μ M of canertininb (n=3). Data are
595 presented as mean \pm SEM; ** = $p < 0.01$. **G** WB representing STAT1 and pSTAT1 in BM-1 cells, following
596 treatment with EGF (50 ng/ml) for 5, 30 and 60 minutes.

Supplementary Table 21. Clinical cases examined in the study. The table provide information about all the meningiomas tested and the level of STAT1 overexpression (gene expression for qPCR and protein expression for WB) detected vs. control. -, HMC=Human Meningeal Cells, L=left; R=right; n/a= not available; M=male; F=female, WB= Western Blot; qPCR= quantitative Polymerase Chain Reaction; IF= immunofluorescence; IHC= immunohistochemistry; Control (STAT1 expression = 1); ~ = STAT1 expression below 2; + = 2/3 times STAT1 overexpression; ++ = 5/6 times STAT1 overexpression; +++ = ≥ 10 times STAT1 overexpression.

ID	Type, Location	WHO	Gender	Age of diagnosis	Analysis	STAT1
Ben Men-1 cells	Benign meningioma cell line	I	F	68	WB, qPCR, IF	+
BTNW71 tissue	Anaplastic, <u>L posterior fossa</u>	III	F	70	qPCR	++
BTNW162 tissue	Anaplastic, <u>L frontal</u>	III	F	76	qPCR	++
BTNW811 tissue	Anaplastic, <u>L posterior fossa</u>	III	F	64	qPCR	++
BTNW831 tissue	Anaplastic, <u>frontal</u>	III	F	68	qPCR	++
BTNW1456 tissue	Anaplastic, <u>L frontal</u>	III	M	48	qPCR	+
MN001 tissue	Atypical, R frontal	II	M	50	IHC, qPCR	+
MN005 cells	Fibroblastic, L posterior fossa	I	F	59	IHC, qPCR	+
MN015 cells	Psammomatous, cervical	I	F	61	WB, qPCR	+
MN017 cells	Transitional, frontal convexity	I	F	51	WB, qPCR, IF	+
MN020 tissue	Atypical, R parietal	II	F	39	qPCR	~
MN023 cells	Meningothelial, L parietal convexity	I	M	63	WB, qPCR	+++
MN028 cells	Transitional, cervical	I	F	63	WB, qPCR, IF	++
MN031 cells	Psammomatous, thoracic	I	F	72	WB, qPCR, IF	++
MN033 cells	Transitional, <u>anterior skull base</u>	I	F	65	WB, qPCR, IF	+
MN036 cells	n/a, R CPA	I	F	51	WB, qPCR	++
MN038 cells	Transitional, L parietal	I	F	79	qPCR	+++
MN045 tissue	Atypical, extra axial parietal	II	M	n/a	qPCR	~
MN048 cells	Fibroblastic, L parietal	I	F	57	WB, qPCR	+++
MN052 cells	Psammomatous, R frontal	I	F	70	qPCR	++
MN054 tissue	n/a, <u>R posterior sinus</u>	I	F	58	qPCR	~
MN055 tissue	n/a, <u>L frontal</u>	I	F	50	qPCR	~
MN056 cells	n/a, R posterior fossa	I	F	61	qPCR	++
MN057 cells	Meningothelial, L parietal	I	M	58	qPCR	+++
MN058 tissue	Angiomatous, R frontal	I	F	65	qPCR	++
MN062 cells	Meningothelial, olfactory groove	I	F	43	qPCR	++
MN066 cells	Psammomatous, <u>thoracicvertebral</u>	I	M	83	qPCR	++
MN071 cells	Secretory/angiomatous, R <u>petroclival</u>	I	F	52	qPCR	++
MN073 cells	Fibroblastic, L convexity	I	F	70	qPCR	++
MN074 cells	Transitional, R angular gyrus	I	F	37	qPCR	+
MN075 tissue/cells	Transitional, R parietal	I	F	79	qPCR	~
MN076 tissue/cells	Atypical, olfactory groove	II	F	53	WB, qPCR	+++
MN077 cells	Transitional, bilateral parasagittal	I	F	66	qPCR	+++
MN078 cells	Transitional, L frontal	I	M	70	qPCR	+++
MN079 tissue/cells	Atypical, occipital	II	M	75	qPCR	~
MN080 cells	Fibrous, L petrous	I	F	64	WB, qPCR	+++
MN082 cells	Fibroblastic, R tentorial	I	F	57	qPCR	+++
MN085 cells	Psammomatous/- fibrous, <u>L frontal</u>	I	F	56	qPCR	+++
MN087 tissue	n/a, CPA	I	M	47	qPCR	~
MN088 tissue	Transitional, sphenoid wing	I	F	n/a	qPCR	~
MN089 cells	Transitional, L parasagittal	I	M	53	qPCR	+++
MN091 cells	n/a, L sphenoid wing	I	F	62	qPCR	+++
MN092 cells	Microcystic, R convexity	I	F	59	qPCR	+++
MN097 tissue	Atypical, L parasagittal recurrent	II	F	66	WB, qPCR	+++
MN101 tissue	Atypical, R frontal	II	F	51	qPCR	++
MN102 cells	n/a, L frontal convexity	I	F	56	qPCR	+++
MN104 tissue	Atypical, R paracentral	II	F	37	qPCR	~
MN105 tissue	Atypical, R frontal	II	F	n/a	qPCR	~
MN106 cells	Psammomatous, <u>planum sphenoid</u>	I	F	46	qPCR	+
MN107 cells	Transitional, R sphenoid wing	I	M	77	qPCR	+++
MN109 cells	Transitional, L posterior frontal	I	F	48	qPCR	+++
MN110 cells	Transitional, L lateral ventricle	I	F	47	qPCR	++
MN113 cells	Secretory, R temporal	I	F	52	qPCR	+++
MN114 cells	Meningothelial, L parasagittal	I	M	62	qPCR	+++
MN115 tissue	Large cystic falcine	I	M	69	qPCR	+
MN125 tissue	<u>Secretory, Left</u> petroclival	I	F	63	qPCR	+++
MN133 tissue	Meningothelial, R fronto-parietal	I	M	87	WB	++
MN139 tissue	Transitional, R sphenoid wing	I	n/a	n/a	qPCR	+
MN140 tissue	n/a, Transitional	I	M	74	qPCR	++
MN148 tissue	Atypical, R frontal	II	M	79	qPCR	~
MN149 tissue	Meningothelial, R frontal	I	n/a	n/a	qPCR	~

Formatted: Indent: Left: 0.1"

Formatted Table

Formatted: Indent: Left: 0.24"

Formatted: Not Highlight

Formatted: Not Highlight

Formatted: Not Highlight

Formatted: Not Highlight

Formatted: Not Highlight

Formatted: Right: -0.29"

ID	Type, Location	WHO	Gender	Age of diagnosis	Analysis	STAT1
MN157 tissue	Meningothelial, extrafrontal	I	F	n/a	qPCR	~
MN168 tissue	Atypica, R-F frontal-occipital	II	n/a	n/a	qPCR	+
MN170 tissue	Meningothelial, frontal parafalcine	I	F	70	WB, qPCR	+
MN176 tissue	Microcystic, L frontal convexity	I	F	43	WB	~
MN180 tissue	Transitional, R occipital lobe	I	F	45	WB, qPCR	++
MN182 tissue	Atypical, R-F fronto-parietal	II	F	66	qPCR	~
MN183 tissue	Chordoid, sellar region	II	F	75	qPCR	~
MN186 tissue	Anaplastic, R temporal	III	M	62	qPCR	~
MN188 tissue	Fibrous, poster fossa	I	F	33	qPCR	~
MN189 tissue	Atypical, left lateral ventricle	II	M	55	qPCR	++
MN194 tissue	Atypical, occipital	II	F	41	qPCR	~
MN196 tissue	Atypical, L parafalcine	II	M	39	qPCR	~
MN200 tissue	Atypical, L fronto-parietal	II	n/a	66	qPCR	+++
MN207 tissue	Psammomatous, thoracic	I	F	n/a	qPCR	~
MN214 tissue	Meningothelial, olfactory groove	I	F	n/a	qPCR	~
MN217 tissue	Fibrous , R tentorial	I	n/a	n/a	qPCR	++
MN219 tissue	Atypical, L fronto-parafalcine	II	M	55	qPCR	~
MN225 tissue	Atypical, L fronto-parafalcine	II	M	57	qPCR	~
MN234 tissue	Atypical, R fronto-parietal	II	F	79	qPCR	+
MN235 tissue	Atypical, R fronto-parafalcine	II	F	71	qPCR	~
MN242 tissue	Fibrous, olfactory groove	I	F	n/a	qPCR	~
MN248 tissue	Mixed Transitional, frontal	I	M	n/a	qPCR	+
MN251 tissue	Fibrous, tentorial	I	F	n/a	qPCR	~
MN252 tissue	Atypical, R parasagittal	II	F	73	qPCR	~
MN261 tissue	Transitional, L parasagittal	I	M	n/a	qPCR	+
MN263 tissue	Atypical, L frontal convexity	II	M	78	qPCR	~
MN274 tissue	Fibrous, L parietal	I	F	68	qPCR	+++
MN278 tissue	Meningothelial, R sphenoid	I	F	n/a	qPCR	+
MN332 tissue	L frontal parafalcine	II	M	68	qPCR	~
MN338 tissue	L temporal convexity	II	F	88	qPCR	++
NH09 tissue	Malignant Anaplastic, occipital	III	n/a	n/a	qPCR	+++
NH10 tissue	Malignant Anaplastic, frontal	III	n/a	n/a	qPCR	+++
J1 tissue	Atypical, sphenoid wing	II	F	62	IHC	++
J2 tissue	Atypical, parafalcine	II	F	51	WB, IHC	++
J3 tissue	Atypical, frontal	II	M	64	WB, IHC	++
J4 tissue	Atypical brain invasion, occipital	II	M	66	WB, IHC, qPCR	+++
J5 tissue	Fibroblastic, occipital	I	F	50	WB, IHC	+++
J6 tissue	Transitional, parasagittal	I	F	37	WB, IHC	+++
J7 tissue	Transitional, parasagittal	I	F	72	WB, IHC	+++
J8 tissue	Transitional, parasagittal	I	F	68	WB, IHC	++
J9 tissue	Malignant, occipital	III	F	82	WB, IHC	++
J10 tissue	Malignant occipital	III	M	85	WB, IHC, qPCR	++
J11 tissue	Malignant, occipital	III	M	85	WB, IHC, qPCR	+++
J12 tissue	Malignant, parasagittal	III	M	87	WB, IHC	++
J22 tissue	Atypical, occipital	II	M	69	qPCR	++
J23 tissue	Atypical, temporal	II	F	62	qPCR	++
#aD1 tissue/#a	Meningothelial	I	n/a	n/a	IHC	+
#aD2 tissue	Meningothelial	I	n/a	n/a	IHC	+
#aD3 tissue	Meningothelial	I	n/a	n/a	IHC	+
#aD4 tissue	Secretory	I	n/a	n/a	IHC	+++
#aD5 tissue	Secretory	I	n/a	n/a	IHC	+++
#aD6 tissue	Secretory	I	n/a	n/a	IHC	++
#aD7 tissue	Secretory	I	n/a	n/a	IHC	+++
D8 tissue/#a	Secretory	I	n/a	n/a	IHC	+++
D9 tissue/#a	Secretory	I	n/a	n/a	IHC	+
D10 tissue/#a	Transitional	I	n/a	n/a	IHC	++
D11 tissue/#a	Mosaic Fibroblastic	I	n/a	n/a	IHC	+
D12 tissue/#a	Fibroblastic	I	n/a	n/a	IHC	++
D13 tissue/#a	Fibroblastic	I	n/a	n/a	IHC	++
D14 tissue/#a	Psammomatous, spinal	I	n/a	n/a	IHC	++
D15 tissue/#a	Atypical	II	n/a	n/a	IHC	++
D16 tissue/#a	Atypical	II	n/a	n/a	IHC	++
D17 tissue/#a	Atypical, brain invasion	II	n/a	n/a	IHC	++
D18 tissue/#a	Atypical, brain invasion	II	n/a	n/a	IHC	++
D19 tissue/#a	Atypical, brain invasion	II	n/a	n/a	IHC	++
D20 tissue/#a	Malignant	III	n/a	n/a	IHC	++
D21 tissue/#a	Malignant	III	n/a	n/a	IHC	+
D22 tissue/#a	Malignant	III	n/a	n/a	IHC	+

Formatted: Indent: Left: 0.1"

Formatted Table

Formatted: Indent: Left: 0.24"

Formatted: Not Highlight

Formatted: Not Highlight

ID	Type, Location	WHO	Gender	Age of diagnosis	Analysis	STAT1
D23 tissue n/a	Malignant	III	n/a	n/a	IHC	+++
D24 tissue n/a	Malignant	III	n/a	n/a	IHC	++
D25 tissue n/a	Malignant	III	n/a	n/a	IHC	+++
HMC	Human meningeal cells	n/a	n/a	n/a	WB, qPCR, IF	Control
BioChain ^{R1234043-10}	Cerebral meninges	n/a	F	82	WB , qPCR	Control
ABS ¹⁵⁰¹⁰²⁴¹⁶	Cerebral meninges	n/a	F	92	WB, qPCR	Control
ABS ⁹⁰²⁰⁰⁰⁰³²¹⁵	Cerebral meninges	n/a	F	78	WB, qPCR	Control
n/aC1	Cerebral meninges	n/a	n/a	n/a	IHC	Control
n/aC2	Cerebral meninges	n/a	n/a	n/a	IHC	Control
n/aC3	Cerebral meninges	n/a	n/a	n/a	IHC	Control
n/C4a	Cerebral meninges- glioma	n/a	n/a	n/a	IHC	Control
n/C5a	Cerebral meninges- glioma	n/a	n/a	n/a	IHC	Control
n/C6a	Cerebral meninges- glioma	n/a	n/a	n/a	IHC	Control
Abcam ^{ab29466}	Brain (human) tissue lysate	n/a	n/a	n/a	WB	+
n/C7a	Normal brain temporal lobe	n/a	n/a	n/a	IHC	Control
n/C8a	Normal brain temporal lobe	n/a	n/a	n/a	IHC	+
n/C9a	Normal brain occipital lobe	n/a	n/a	n/a	IHC	Control
n/C10a	Normal brain frontal lobe	n/a	n/a	n/a	IHC	Control

Formatted: Indent: Left: 0.1"

Formatted Table

Formatted: Indent: Left: 0.24"

Supplementary Table 42. Complete list of the antibodies employed in the study, their application and the concentrations used. WB: Western Blot; IF: Immunofluorescence; IP: Immunoprecipitation; IHC: Immunohistochemistry.

Antibody	Manufacturer	Application	Dilution
STAT1	Cell Signaling Technology - #9172 Santa Cruz Biotechnology - sc-592	WB	1:1000
		WB	1:1000
		IF	1:300
		IHC	1:150
pSTAT1-Y701	Abcam - ab29045 R&D Systems - AF2894 Cell signalling - #7649	WB	1:500
		IF	1:100
		WB	1:1000
		IHC	1:200
		WB	1:500
pSTAT1-S727	Cell Signaling Technology - #9177	IP	1:50
		WB	1:1000
		IF	1:100
JAK1	Cell Signaling Technology - #3344	IHC	1:400
		WB	1:1000
		WB	1:500
pJAK1- Y1022/1023	Cell Signaling Technology - #3331	WB	1:500
JAK2	Cell Signaling Technology - #3230	WB	1:1000
pJAK2- Y1007/1008	Cell Signaling Technology - #3771	WB	1:500
TYK2	Cell Signaling Technology - #14193	WB	1:500
pTYK2- Y1054/1055	Cell Signaling Technology - #9321	WB	1:500
IFN γ	Abcam - ab25101	WB	1:500
CD163	Bio-Rad - MCA1853	WB	1:500
Merlin	Cell Signaling Technology - #6995	WB	1:1000
pMerlin- S518	Cell Signaling Technology - #9163	WB	1:500
ERK	Cell Signaling Technology - #4695	WB	1:2000
pERK- T202/204	BD Biosciences - #612358	WB	1:500
AKT1	Cell Signaling Technology - #4691	WB	1:1000
pAKT1- S473	Cell Signaling Technology - #9271	WB	1:500
RB	Cell Signaling Technology - #9309	WB	1:2000
pRB- S780	Cell Signaling Technology - #8180	WB	1:1000
CD63 (MEM-259)	Thermo Fisher Scientific - MA119281	IF	1:250
CD63	Cambridge Bioscience - EXOAB-CD63A-1	WB	1:500
CD9 (C-4)	Santa Cruz Biotechnology - #13118	IF	1:250
CD9	Cell Signaling Technology - #13174	WB	1:500
GM130	BD Transduction Laboratories - #610823	WB	1:1000
Calnexin (H-70)	SantaCruz Biotechnology - #11397	WB	1:1000
CyclinD1	Cell Signaling Technology - #2978	WB	1: 300
Ki67 (MIB-1)	DAKO - #M7240	IF	1: 1000
PIAS1	Cell Signaling Technology - #3550	WB	1:1000
PIAS3	Cell Signaling Technology - #9042	WB	1:1000
PIAS4	Cell Signaling Technology - #4392	WB	1:1000
SOCS1	Cell Signaling Technology - #3950	WB	1:1000
SOCS2	Cell Signaling Technology - #2779	WB	1:1000
SOCS3	Cell Signaling Technology - #2932	WB	1:1000
EGFR	Cell Signaling Technology - #4267	WB	1:1000
pEGFR- Y1068	Cell Signaling Technology - #3777	WB	1:500
pP70 S6K – T421/S424	Cell Signaling Technology - #9204	WB	1:500
P70 S6K	Cell Signaling Technology - #9202	WB	1:500
GAPDH	EMD Millipore – MAB374	WB	1:50000

Figure 1

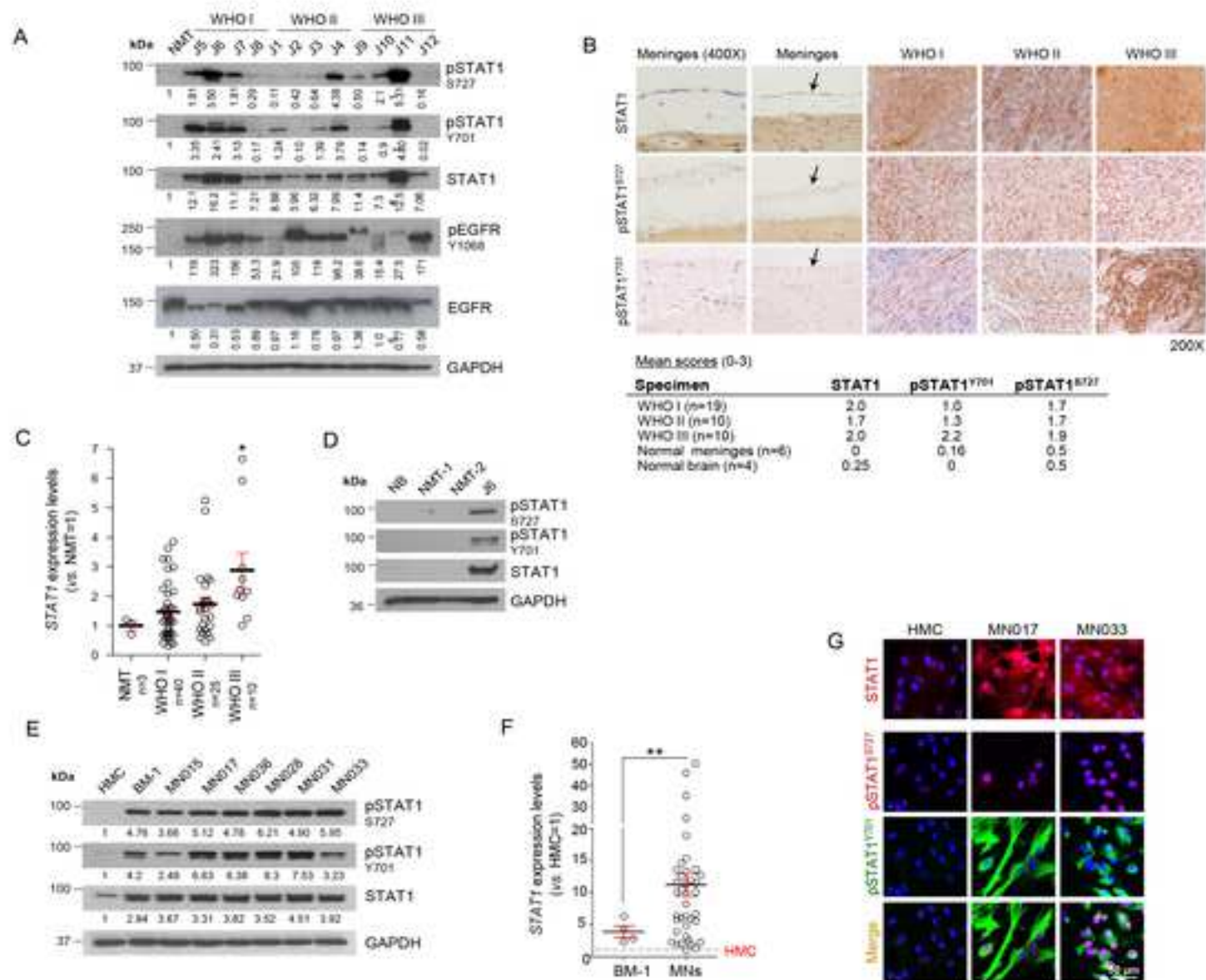


Figure 2

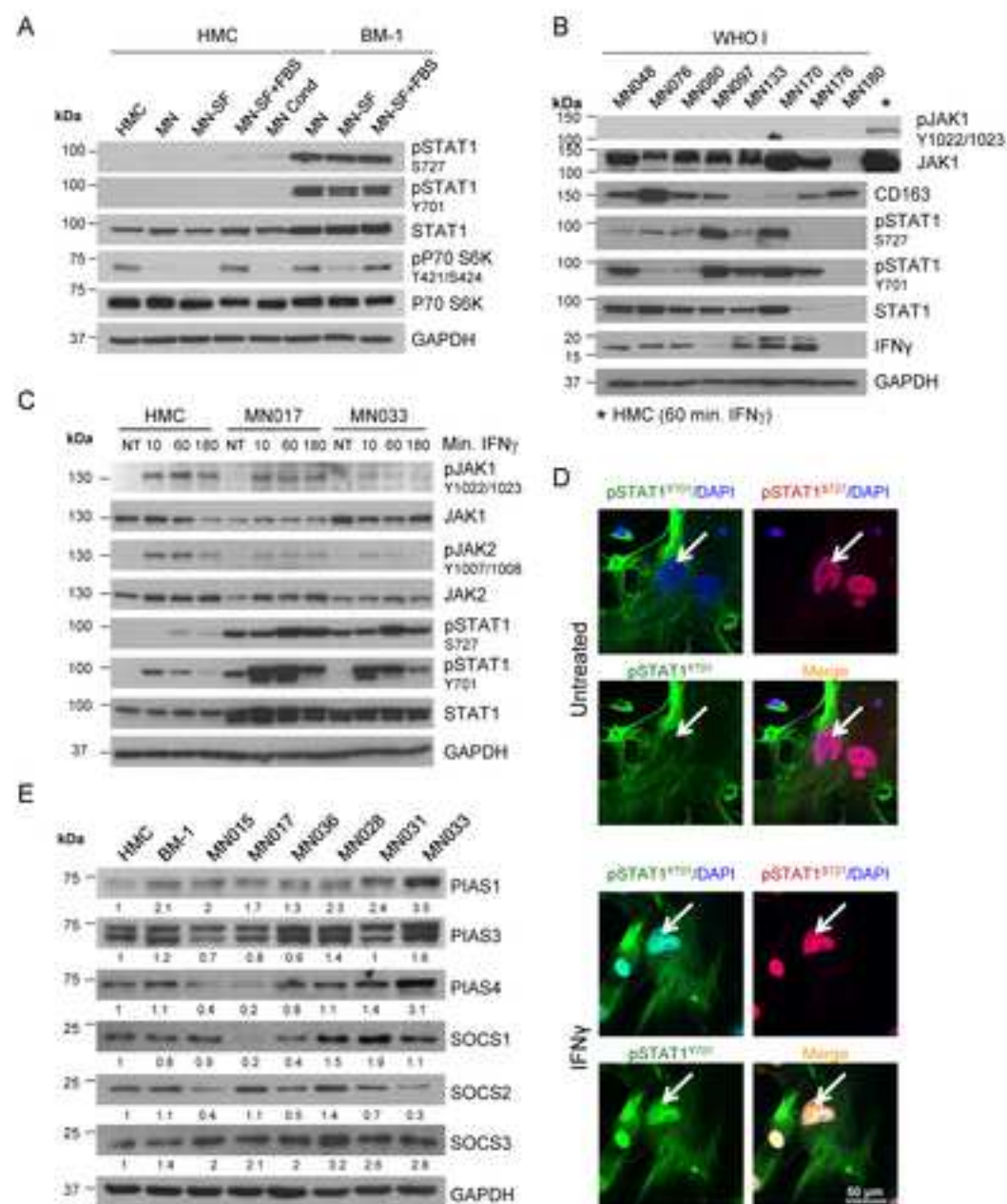


Figure 3

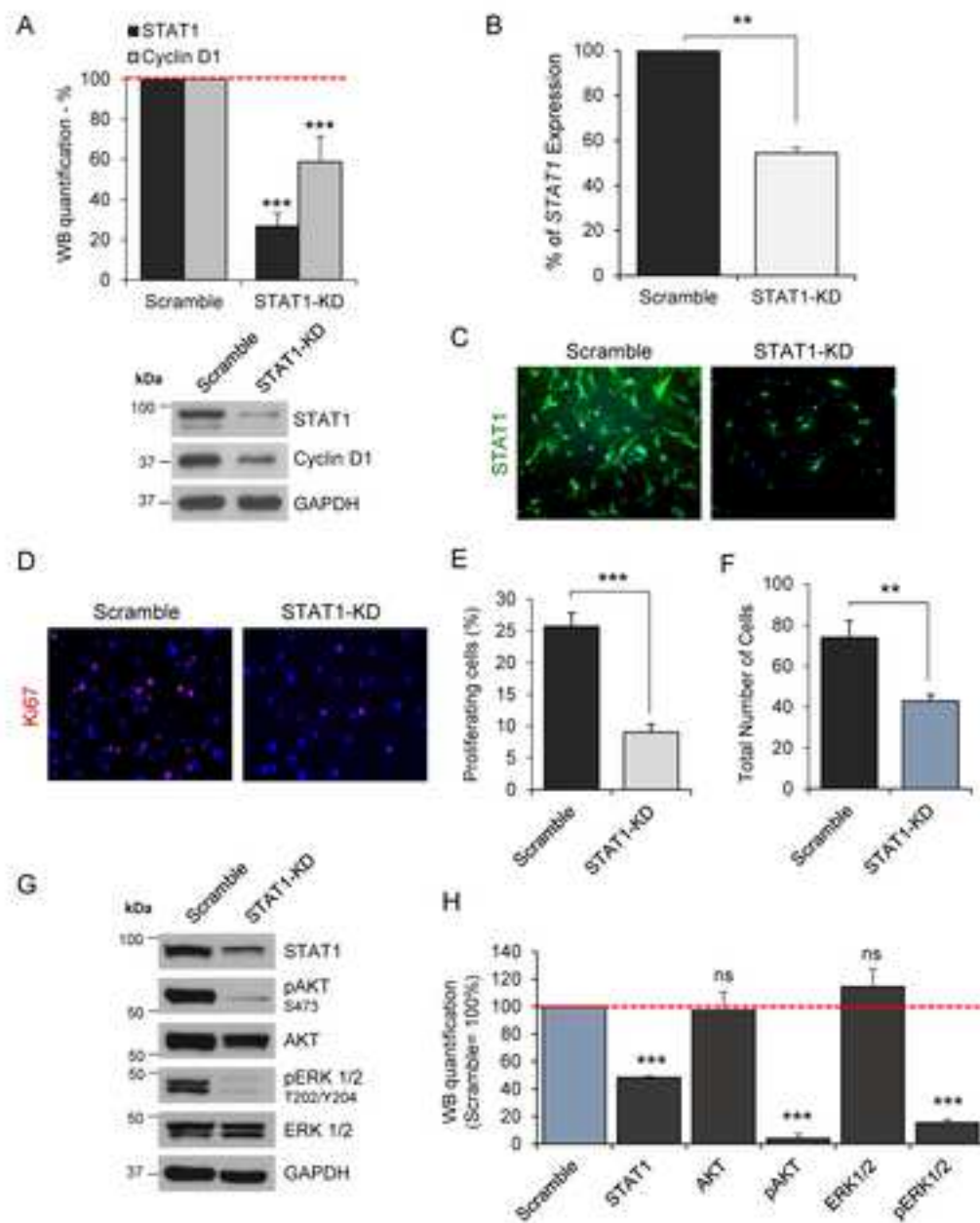


Figure 4

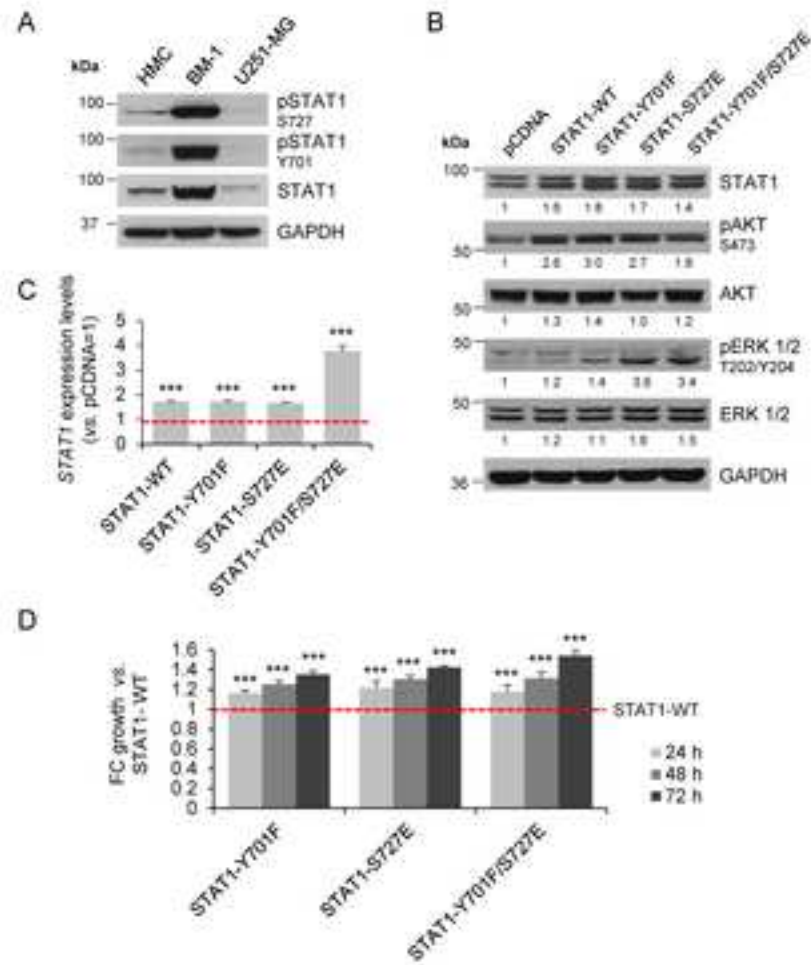
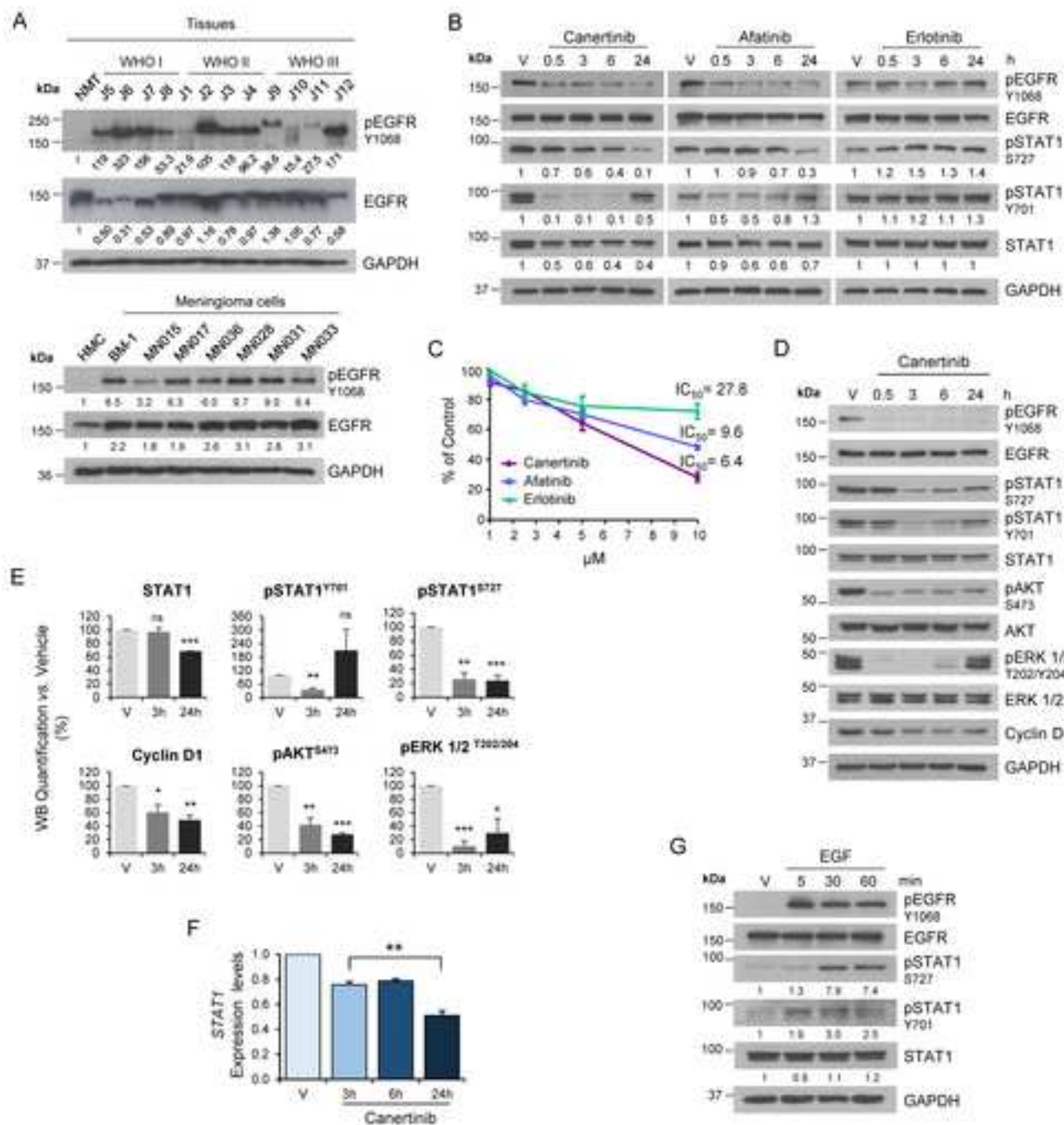
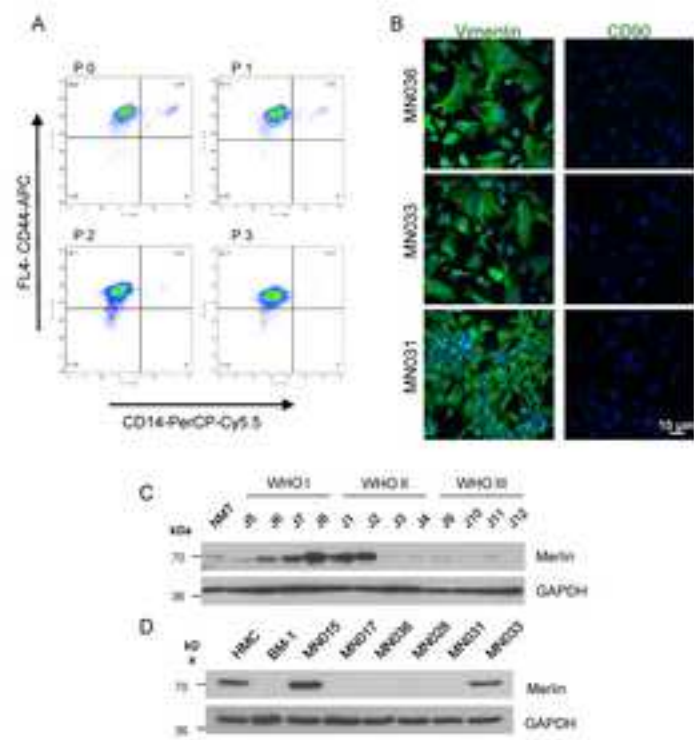


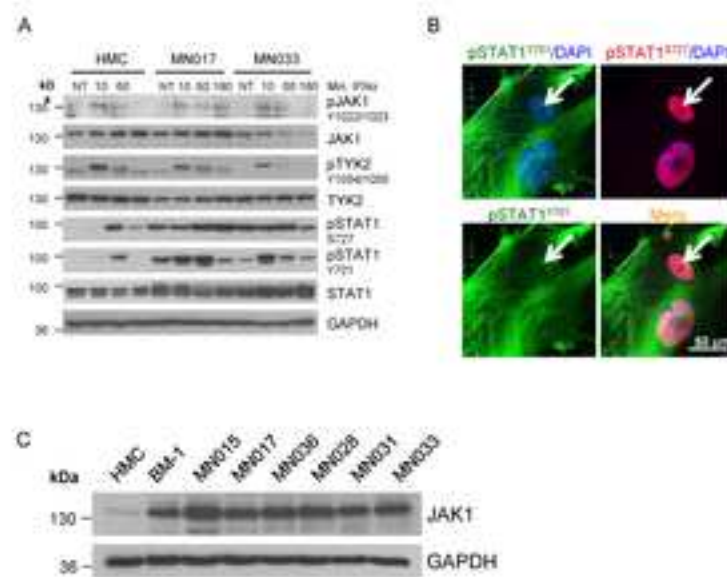
Figure 5



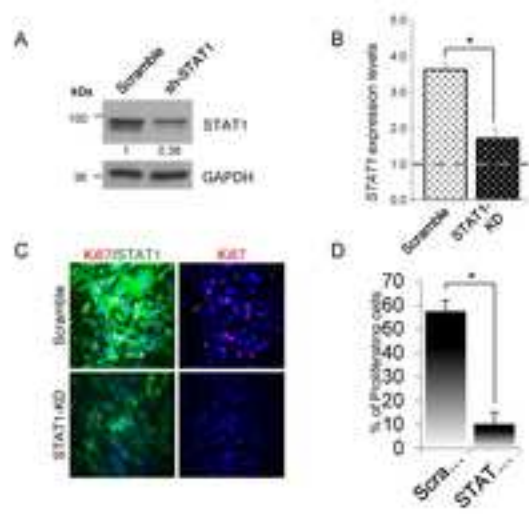
Supplementary Fig. 1



Supplementary Fig. 2



Supplementary Fig. 3



Supplementary Fig. 4

	Caerdocic				Caerdocic				Caerdocic						
42	V	05	3	6	V	05	3	6	24	V	05	3	6	24	Hours
100	[Bar chart]				[Bar chart]				[Bar chart]				pEGFR Y1068		
100	[Bar chart]				[Bar chart]				[Bar chart]				EGFR		
100	[Bar chart]				[Bar chart]				[Bar chart]				pSTAT1 S377		
100	[Bar chart]				[Bar chart]				[Bar chart]				pSTAT1 Y326		
100	[Bar chart]				[Bar chart]				[Bar chart]				STAT1		
90	[Bar chart]				[Bar chart]				[Bar chart]				pAKT S473		
90	[Bar chart]				[Bar chart]				[Bar chart]				AKT		
90	[Bar chart]				[Bar chart]				[Bar chart]				pERK 1/2 T202/Y204		
90	[Bar chart]				[Bar chart]				[Bar chart]				ERK 1/2		
97	[Bar chart]				[Bar chart]				[Bar chart]				Cyclin D1		
97	[Bar chart]				[Bar chart]				[Bar chart]				GAPDH		
	MN031				MN033				MN036						

1 **Supplementary Figure Legends**

2

3 **Supplementary Fig. 1** Purity of primary meningioma cultures and genetic background of our cohort of samples.

4 **A** Representative flow cytometry analysis of primary MN cells. Dot plots show 10,000 live cells and represent

5 monocyte marker, CD14-PerCP-Cy5.5 (FL3 channel) and potential meningioma tumour marker, CD44-APC (FL4

6 channel). Upper right quadrant represents CD14+ CD44+ phenotype and decreases with passage number (CD14+

7 CD44+ % = Passage 0-4.6, Passage 1-2.1, Passage 2-0.1, Passage 3-0.2). Data analysed was performed on Flow

8 Jo version10.0. **B** Representative confocal images of three primary MN cells tested at passage 3, homogeneously

9 positive for the meningioma marker vimentin (green), while negative for the fibroblast marker CD90. Scale bar

10 10 µm. Nuclei were stain with DAPI (blue). **C** WB analysis showing the expression of Merlin in different grade

11 meningiomas vs. NMT; Next Generation Sequencing (NGS) confirmed that only samples J8, J1 and J2 were

12 Merlin-positive not having any mutation on *Merlin* or loss of heterozygosity (LOH). **D** WB showing the expression

13 of Merlin in in BM-1 and tumour-derived MN cells vs. HMC.

14 **Supplementary Fig. 2** The JAK/STAT pathway in meningioma cells can be activated by IFN α . **A** WB analysis of
15 STAT1 and pSTAT1 (Y701 and S727) protein levels in HMC and two primary MN cells, after IFN α treatment at the
16 concentration of 50 ng/ml for the indicated amount of time. Phospho-JAK1 and pTYK2 are shown to confirm the
17 activation of the JAK/STAT pathway. **B** Representative confocal z-stack images showing localization of pSTAT1-
18 Y701 (green) and pSTAT1-S727 (red) in primary MN cells before and after IFN α stimulation (50 ng/ml for 1 h).
19 Scale bar 50 μ m. Nuclei were stain with DAPI (blue). **C** Representative WB conducted in primary MN cells showing
20 higher levels of JAK1, when compared to HMC.

21 **Supplementary Fig. 3** STAT1 knocked-down reduces proliferation of BM-1 meningioma cells. **A** WB analysis
22 showing the reduction in STAT1 protein levels after *STAT1* sh-RNA-mediated silencing compared to scramble
23 control. **B** Reduction in *STAT1* gene expression associated to *STAT1* sh-RNA-mediated silencing compared to
24 scramble control. Data are presented as mean \pm SEM; * = $p \leq 0.05$. **C** Representative images of the
25 immunofluorescent staining of STAT1 (green) and the proliferation marker Ki67 (red) after *STAT1* sh-RNA-
26 mediated silencing compared to scramble control. Nuclei are stain with DAPI (blue). **D** Histogram presenting the
27 statistical reduction of proliferating cells after STAT1-KD compared to scramble control. Data are presented as
28 mean \pm SD; * = $p \leq 0.05$.

29 **Supplementary Fig. 4** WB quantification after canertinib treatment in primary MN cells. Detailed WB
30 quantification for the histograms presented in Fig 5E. Protein expression was quantified after
31 normalising for the corresponding GAPDH amount and is presented as fold change of the vehicle-
32 treated sample (V).

33